DRL 59
DRD SE-10

DOE/JPL-954887-79/5
Distribution Category UC-63

LSA LARGE AREA SILICON SHEET TASK CONTINUOUS CZOCHRALSKI PROCESS DEVELOPMENT

Texas Instruments Report No. 03-79-10

Final Report

JPL Contract No. 954887
February 1979

Samuel N. Rea

Texas Instruments Incorporated
P.O. Box 225012
Dallas, Texas 75265

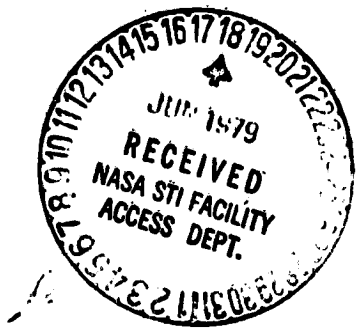

The JPL Low-Cost Silicon Solar Array Project is sponsored by the U.S. Department of Energy and forms part of the Solar Photovoltaic Conversion Program to initiate a major effort toward the development of low-cost solar arrays. This work was performed for the Jet Propulsion Laboratory, California Institute of Technology by agreement between NASA and DOE.

ABSTRACT

A commercial Czochralski crystal growing furnace was converted to a continuous growth facility by installation of a small, in-situ premelter with attendant silicon storage and transport mechanisms. The premelter was situated immediately over the primary melt and provided a molten silicon flow into the large crucible simultaneously as crystal was being grown.

The key element in this continuous Czochralski process is the premelter and a substantial portion of the program involved its evolution into a workable design. The best arrangement tested was a vertical, cylindrical graphite heater containing a small fused quartz test tube liner from which the molten silicon flowed out the bottom. Approximately 83 cm of nominal 5-cm diameter crystal was grown with continuous melt addition furnished by the test tube premelter. High-perfection crystal was not obtained, however, due primarily to particulate contamination of the melt. A major contributor to the particulate problem was severe silicon oxide buildup on the premelter which would ultimately drop into the primary melt. Elimination of this oxide buildup will require extensive study and experimentation and the ultimate success of continuous Czochralski depends on a successful solution to this problem.

Economic modeling of the continuous Czochralski process utilized the IPEG option of SAMICS. The influence of both crystal size and total furnace run size were examined. Results of these studies indicate that for 10-cm diameter crystal, 100-kg furnace runs of four or five crystals each are near optimal. Costs tend to asymptote at the 100-kg level so little additional cost improvement occurs at larger runs. For these conditions, crystal cost in equivalent wafer area of around $\$16/m^2$ exclusive of polysilicon and slicing is obtained. Lower crystal costs can be obtained by growing larger diameter crystal in the 12 to 15-cm range. The outlook for achieving the overall 1986 wafer cost goals is not optimistic because of high slicing costs. Continuous Czochralski can, however, meet the near-term cost goals for silicon sheet material.

TABLE OF CONTENTS

LIST OF ILLUSTRATIONS

LIST OF TABLES

CONTINUOUS CZOCHRALSKI PROCESS DEVELOPMENT

Texas Instruments Incorporated

Final Report

SECTION I
INTRODUCTION

This program addressed the feasibility of a continuous Czochralski process employing liquid silicon melt replenishment during growth. An incoming flow of solid granular or nugget polysilicon was premelted in a small auxiliary crucible from which liquid silicon was introduced into the main or primary crucible. Liquid melt addition rather than solid addition was pursued because this replenishment technique causes minimal thermal and mechanical disturbances to the primary melt.

Continuous Czochralski is defined here as the growing of several crystals from a single liner with continual melt replenishment during growth. The process is interrupted periodically in order to remove completed crystals after they have grown to some maximum predetermined size. During crystal removal, the hot zone is maintained under power with the silicon in the crucible remaining molten.

Silicon crystal grown by the Czochralski technique (Cz silicon) is a well-established process providing over 90% of the single crystal wafers utilized by the worldwide semiconductor industry. This large market base has resulted in continual improvements in Cz furnaces until current 20-kg batch pull machines represent a fairly mature technology. However, silicon sheet produced by today's batch Cz process will not meet the mid 1980's cost goals for solar cell material. There are several, fairly obvious, reasons for this of which Cz ingot slicing represents a sizable cost element as does the polysilicon starting material for Cz growth. Both these cost elements are being attacked through several programs in the JPL LSA Project and will not be discussed further in this report other than to make reasonable assumptions regarding cost goals of these efforts.

The Czochralski process is materials and capital intensive. Current Cz add-on cost (i.e., 1979 costs exclusive of polysilicon, slicing, and profit) for 10-cm crystal pulled in the batch made at 100% crystal yield is around $61/m^2. Table 1 gives a breakdown of this cost computed by the IPEG Price Equation of SAMICS.[1] Materials and capital account for 84% of the total cost with crucible liners alone representing nearly a third of the total. Obviously, if a crucible liner could be reused only once, then a 15% cost savings could be realized immediately. Thus, it is apparent that to decrease Czochralski costs, it is necessary to increase the crystal output per furnace run assuming the various cost elements in Table 1 do not escalate faster than the output.

Costs in Table 1 are expressed in dollars per square meter of silicon sheet. The conversion factor from Cz ingot to slices used was 16 slices per cm of ingot length. This represents a yielded

Table 1. Czochralski Crystal Add-On Costs (Batch Pull, 20 kg Charge, 100% Yield)

Cost Category	Cost	% of Total
Capital	$10.44/m^2	17.1%
Direct Labor	4.92	8.1
Crucible Liners	18.48	30.3
Other Materials	22.49	36.8
Miscellaneous	4.73	7.7
	$61.06/m^2	100.0%

slice plus kerf thickness of 0.63 mm which is current state-of-the-art for both ID sawing and multi-blade slurry slicing. Of course the costs in Table 1 are inversely proportional to the ingot-slice conversion rate. The sawing goal for the 1982 time frame is 25 slices/cm ingot length at 95% yield[2,3] for a net of 23.75 slices/cm. With 10-cm diameter crystal, this sawing goal results in a convenient 1 m^2 sheet/kg ingot. The application of the 1982 goal to the costs in Table 1 results in a 30% cost reduction to $41.14/m^2 Cz add-on cost..

Three approaches are available to increase the crystal output per furnace run: (1) multicharging in which polysilicon is added to the crucible between ingots, (2) continuous growth with crucible silicon addition (solid or liquid) during growth, and (3) utilize super-large crucibles and pull several crystals from the one pot: multipulling. Experience with multicharging[4] indicated that impurity buildup, especially carbon, is likely to be a controlling factor resulting in high-dislocation or even polysilicon growth after a few ingots. Similarly, multiple crystals pulled from a single large charge would also exhibit a serious impurity buildup which would adversely affect crystal quality.

In view of these fundamental physical difficulties inherent in multicharging or multipulling, a continuous Czochralski process was selected for developmental work since continuous Cz offers the lowest potential crystal cost as well as a number of technical advantages over competing approaches:

1. Uniform Crystal Resistivity: Continuous melt replenishment with doped polysilicon feed provides a constant dopant concentration in the melt. Thus, resistivity will be uniform along the length of each crystal and no yield loss due to resistivity will occur.

2. Slice-to-Slice Uniformity: In addition to axial resistivity uniformity, crystal-to-crystal uniformity would be greatly enhanced since large polysilicon lots uniformly doped could supply many continuous runs. In a continuous process, each crystal would experience the same thermal history and pull rate so that slices cut from these crystals would be virtually identical. Consequently, solar cell processing could be optimized and standardized for maximum efficiency and processing economics.

3. Faster Pull Rates: A continuous process can provide faster pull rates than batch processes.[4] Faster pulls not only lower crystal costs by improving productivity but there is some evidence that faster pulls result in flatter growth interfaces and lower radial resistivity gradients.

4. Improved Temperature Control: Once thermal stability is attained in a continuous run, it is much easier to maintain optimal melt temperature since the crucible remains stationary during a pull.

5. Higher Productivity: Not only does the faster pull rate contribute directly to higher production rates but the dead times associated with batch melt-ins can be eliminated. Thus, total cycle time to produce a given crystal weight can be shortened and overall puller utilization increased.

6. Lower Crystal Cost: The higher productivity of a continuous process contributes directly to lower crystal cost provided puller depreciation and maintenance are not excessive. Current projections indicate that depreciation (or puller price) and maintenance can be held to acceptable levels. Another factor resulting in lower cost is the inherently higher crystal yields a continuous process can provide. Stable thermal conditions will provide good crystal diameter control so grind losses will be minimized. Also, uniform crystal resistivity will eliminate this potential yield loss. Various cost projections are given in Section III.

The approach to a continuous Cz furnace pursued in this program was predicated on several common-sense guidelines deemed appropriate for a new generation of pullers:

1. Minimal Furnace Component Count: This reduces capital costs as well as reduces subsequent spares inventory costs.

2. Low-Complexity, Low-Cost Components: Keep things simple and inexpensive to minimize operating costs and provide high reliability for extended furnace runs.

3. Easy Maintenance: This should follow as a natural consequence of a low components count coupled with simplified, straightforward designs.

4. Low Energy Consumption: A continuous puller should be less energy intensive than a batch charge furnace due to greater productivity per run. However, care must be exercised in designing the auxiliary premelter to ensure that this energy advantage is maintained.

5. Minimal Equipment Size: This is to lower equipment and building amortization and occupancy costs.

In keeping with these general design guidelines, Texas Instruments constructed a furnace along the lines illustrated in Figure 1. A Varian 2848A puller was modified extensively to permit continuous silicon feed. Modifications included a new lower chamber, addition of a high-temperature vacuum valve, and a modified upper chamber to accept a Hamco cable seed-pull mechanism equipped with crystal weight readout. In addition, the polysilicon storage and feed components depicted in Figure 1 were constructed. The vibratory hopper supplies granular, chunk, nugget, or

fine polysilicon to an auger feed. A variable speed auger drive transports the silicon to a melt station where the polysilicon is melted in an auxiliary crucible and then flows into the primary crucible. The furnace operates under vacuum with argon purge.

All the components in the continuous furnace are either off-the-shelf items or fairly straightforward in design. The major technical obstacle in this program was design of a suitable auxiliary crucible/melter (premelter) which is discussed in detail in Section II.

SECTION II
TECHNICAL DISCUSSION

A. FURNACE DESIGN AND CONSTRUCTION

Figure 1 shows the basic continuous Cz furnace elements. Brief descriptions are given below of the various designs and modifications made to the Varian 2848A to enable continuous operation.

1. Lower Dome

A new lower chamber was designed and built to accept the vacuum valve, auger feed, and auxiliary melter. A flat-top chamber was utilized in order to minimize overall puller height. The chamber is double-wall construction with water cooling. A 25-cm (10-inch) diameter side appendage 13 cm (5 inches) long was integral with the lower chamber to provide room for the auger feed and auxiliary melter. Engineering drawings of the chamber are contained in Appendix A.

2. Upper Chamber

The existing upper chamber of the Varian 2848A furnace was utilized with the addition of transition sections designed and built to mate the vacuum valve and to attach the Hamco cable pull mechanism. Other minor modifications were effected in order to use the existing chamber lift mechanism.

3. Auger Feed

A commercial auger was purchased from Thomas Conveyor of Fort Worth, Texas. The auger was 76-mm ID and approximately one meter long and constructed of stainless steel. It was driven by a 3/4 hp variable speed dc motor purchased from Hampton Products in Rockford, Illinois. The auger assembly was vacuum-tight being sealed at the motor end by a dual O-ring design having intermediate vacuum pumping. This O-ring arrangement proved to be virtually leak-free in operation.

4. Silicon Hopper

The hopper was constructed of stainless steel and designed to hold 100 kg of silicon fines whose average density is approximately 40% that of solid silicon. The hopper lid is aluminum with an O-ring seal at the top flange. An Eriez Magnetic vibrator was attached to the conical exit section to prevent material clogging. Details of the hopper are in Appendix A.

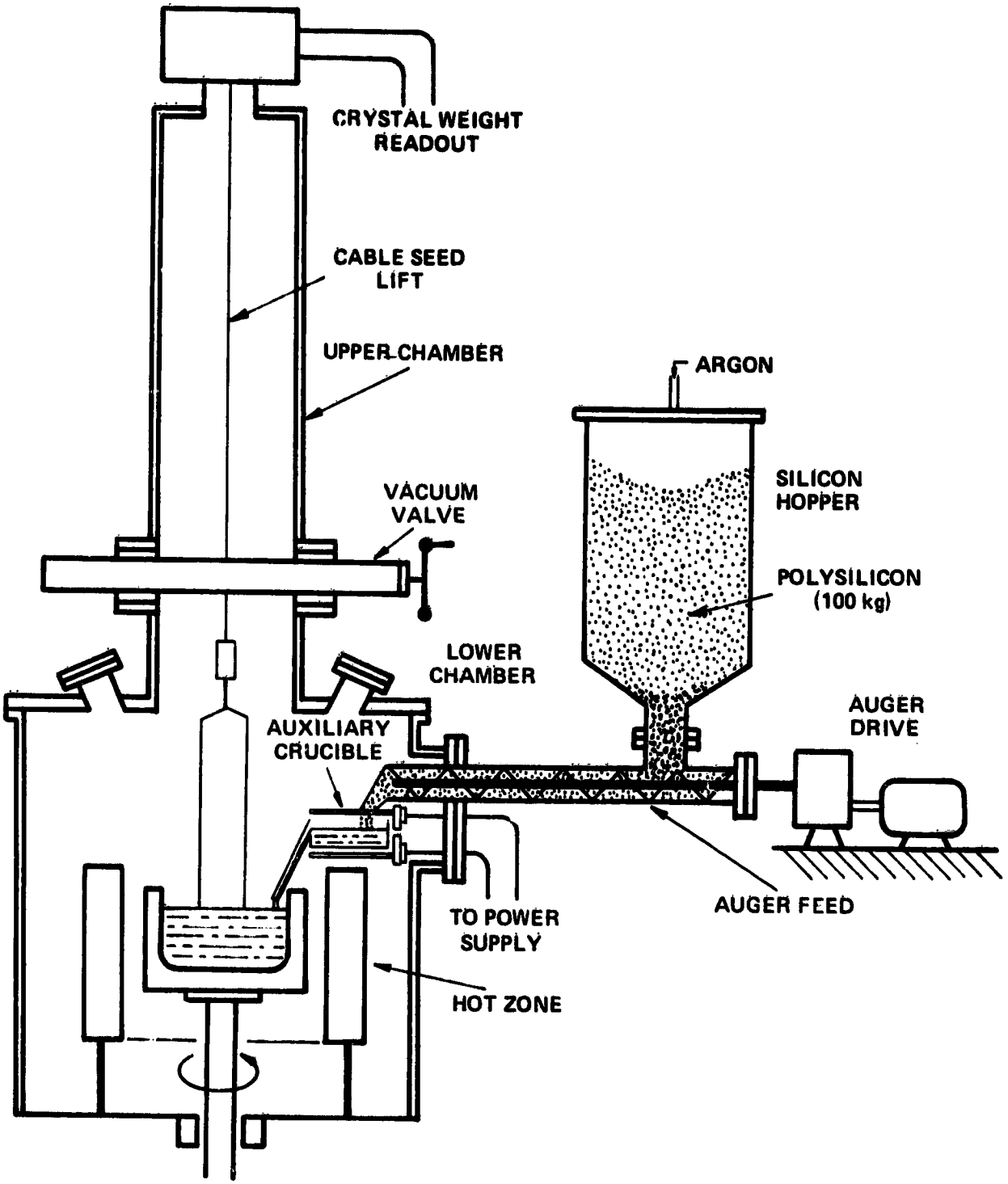

Figure 1. Continuous Czochralski Silicon Furnace

A careful assessment of the heater, heat shield package, and chamber space available indicated that the standard Varian 2848A 12-kg configuration was adequate. Thus, no modifications to the hot zone were made.

6. Miscellany

The stainless steel vacuum valve between the lower and upper chamber was water-cooled and pneumatically operated. Throat diameter was 15 cm. The valve was manufactured by VAT of Switzerland and was purchased through HPS Corporation in Denver, Colorado.

The Hamco cable pull seed lift was purchased with the crystal weight readout option to enable melt level control. The calibrated auger feed rate could be adjusted to balance the rate of crystal withdrawal thereby maintaining a stationary melt level. No active feedback control was installed.

An auxiliary control panel for the melter, hopper, auger, and crystal weight controls and readouts was constructed. This panel was attached to the top of the existing Varian puller control console.

The various puller parts, with the exception of the indicated purchased items, were fabricated in the internal Texas Instruments machine shops.

B. PREMELTER DEVELOPMENT

1. Premelter Power Requirement

One of the goals of a continuous Cz process is to grow 10-cm diameter crystal at 10 cm/h. At these growth conditions, 1838 g/h of polysilicon will be converted to crystal and this quantity must be supplied by the premelter. For estimation purposes, it is assumed that 1900 g/h of silicon will be converted from a solid at room temperature to a liquid stream at the melting point of 1412°C. The heat required is given by:

$$Q = \dot{m}\, c\, (T_{melt} - T_{room}) + \dot{m}\, h_{if} \qquad (1)$$

in which

Q = heat required, W

$\dot{m}$ = silicon flow rate, 1900 g/h

c = average silicon specific heat, 917 J/kg-K

T_{melt} = 1412°C

T_{room} = 25°C

h_{if} = silicon heat of fusion, 1810 J/g

With the conversion constant 1 joule = 1 watt-second, eq. (1) gives

$$Q = 671\ W + 955\ W = 1626\ W.$$

Thus, a minimum premelter power of approximately 1.6 kW is required to melt the incoming solid silicon stream.

This calculation neglects any heat losses in the process. Very early premelter work indicated a power requirement around 6 kW would be necessary to overcome the various heat losses and provide sufficient heat to melt the silicon flow. Consequently, a 9-kW power supply was purchased to provide a safety margin. In actual practice, however, it was determined that with adequate premelter insulation only 3-4 kW was sufficient for the test tube premelter design finally adopted.

2. Premelter Experiments

The premelter design was the key technical challenge in the continuous puller concept depicted in Figure 1. In fact, this program in essence became a premelter development program. In designing the lower dome of Figure 1, it was assumed that a horizontal premelter configuration would be possible. However, as premelter development progressed in parallel with puller design, it became obvious that a horizontal arrangement would not work, but, of necessity, the puller design was frozen and under construction at that point. Consequently, the final, vertical premelter was not a perfect complement to the puller lower dome design.

Initial experiments to determine a workable premelter design utilized a small RF power supply operating at 5 MHz. At this frequency, it was not possible to load directly into small polysilicon nuggets so a graphite sleeve was placed over the quartz tube crucible to provide a load for the RF power. Some success was achieved in melting silicon using this setup. A careful assessment of the pros and cons of RF power indicated, however, that a RH (resistance-heated) auxiliary crucible had many advantages. For instance, initial cost is lower, heater design is simpler, and maintenance is considerably less for a RH power supply as opposed to a RF design. Consequently, subsequent work focused on RH auxiliary crucibles.

A laboratory-scale experimental setup was assembled to test various premelter configurations. This work was done in a small sand quartz reactor tube 24-cm ID by 46-cm long under a 1-atm argon ambient. A 400-A, 12-V power supply was utilized. The first design tested was a vertical split-tube configuration shown in Figure 2 fabricated from high-density purified graphite. The tube OD was 2.5 cm, the silica liner ID was 1.0 cm, and overall length was 20 cm. The original design had a 3-mm orifice in the base of the liner and silicon was caused to flow from the tube by pressurizing with argon while granular silicon fines were being added. The flow of material through the orifice, even with larger openings, was never controllable due to the high surface tension of the melt. The major limitation was that of achieving a sufficiently high temperature to assure maximum fluidity of the melt.

A half-tube resistive element design was then tested with a fused silica boat positioned horizontally as shown in Figure 3. Inside diameter of the heater was 5.0 cm and length was 15 cm. The maximum available power input to the element (4.8 kW) was barely sufficient to melt the silicon

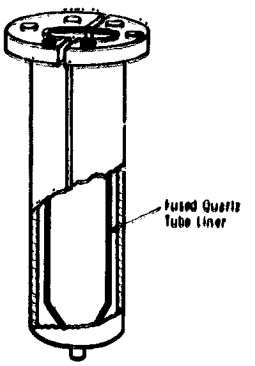

Figure 2. Test Tube Premelter

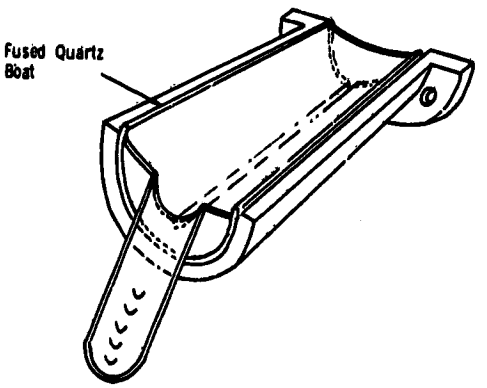

Figure 3. Half-Tube Premelter Design

and insufficient to cause the melt to flow from the spout. Again, the temperature achieved was only slightly above the silicon melting point. A large amount of heat was lost to the environment and the chamber containing the heating element was inadequately sealed and purged to completely eliminate oxygen back-diffusing into the system. The "dross" or skin formed on the melt surface greatly inhibited melt flowability.

The half-tube design of Figure 3 was carried one step further to the cylindrical design of Figure 4. This cylindrical design provided substantially greater temperatures in the silicon since the graphite heater served as its own heat shield. Dimensions of the heater were approximately the same

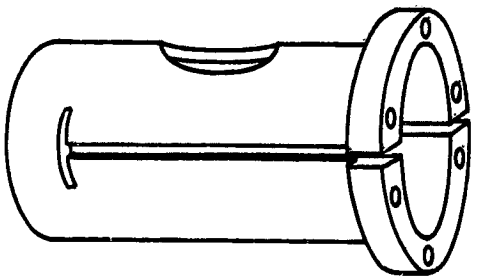

Figure 4. Auxiliary Crucible Heater: Split Tube Design

as the half-tube; 5 cm ID by 16 cm long. The quartz boat of Figure 3 was placed inside the heater to serve as a crucible. The premelter was wrapped with several layers of graphite felt for additional insulation and no problems were encountered in achieving melts with approximately 4 to 4.2 kW power input. However, melt solidification in the crucible exit spout prevented good liquid flow from the crucible. Also, extreme devitrification of the fused quartz boat was observed due to the high temperatures achieved in efforts to effect silicon flow.

The Figure 4 premelter configuration was then altered slightly to utilize quartz boats containing a vertical exit spout in the bottom extending through a hole in the graphite heater. This arrangement was successful in providing molten flow from the premelter. However, the nonwetting of the fused quartz by the molten silicon caused the silicon to ball up and not flow out of the crucible in a continuous stream. Instead, the silicon exited the crucible in discrete globules or droplets.

The most straightforward approach to overcoming the nonwetting and devitrification associated with fused quartz crucibles is to eliminate the crucible altogether. This was tried by making an integral heater/crucible using the Figure 4 heater design. Graphite end plates were glued to the heater using Dylon GC graphite cement. A graphite exit nozzle was screwed into a threaded hole drilled through the bottom of the heater and the entire assembly was SiC-coated. This crucible is illustrated in Figure 5.

Results in laboratory tests with the integral heater/crucible were moderately encouraging. The intimate contact between silicon and heater provided rapid, efficient melting and the exit flow more nearly resembled a stream than did the previous approaches. However, some plugging in the exit nozzle was observed due to inadequate power available from the small power supply. The thermal environment in the test chamber was quite different from that of a puller under power and operating at 20-mm Hg pressure. Consequently, it was decided to discontinue premelter development work in the test chamber and begin using the continuous puller which was now completed and ready for testing.

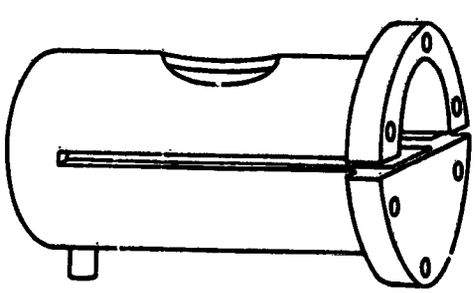

Figure 5. Integral Auxiliary Heater/Crucible

The various technical and operational difficulties uncovered in laboratory work with the horizontal premelter configurations of Figures 3-5 caused a reevaluation of the "test tube" premelter design of Figure 2. This design offers several advantages over the horizontal configurations: (1) the heater is relatively easy to fabricate, (2) heating is efficient, (3) the premelter can be positioned directly over the primary melt and in close proximity to minimize melt-splashing, and (4) minimal premelter insulation is required since the primary crucible and melt provide a built-in thermal barrier to heat losses. Thus, the premelter approach illustrated in Figure 2 was selected for testing in the continuous puller.

The machined graphite heating element had a 38-mm ID and was 140-mm long. Initial testing utilized either SiC-coated or bare graphite so that the heater formed its own crucible. The auxiliary power supply for the continuous puller premelter could provide 9 kVA (600 A at 15 V) and this power was supplied to the premelter through water-cooled copper electrodes bolted to the premelter top flange with tantalum bolts. In early tests, the premelter was positioned 30 degrees from vertical, angled into the primary crucible. Silicon fines were fed into the open top by the auger feed system. The primary crucible was loaded with 4-kg silicon which was maintained in the molten state during premelter testing. No attempts were made to grow crystal while testing the premelters.

Several experimental runs were made at first with the bare graphite heaters. These runs showed feasibility in that the incoming silicon could be melted and caused to flow into the primary crucible. However, the molten silicon reacted rapidly with the bare graphite premelter and the large volume expansion which occurs when silicon reacts with graphite to form SiC caused severe cracking of the heater. Once the heater cracked, electrical continuity was lost and the heater cooled down below the silicon melting point thereby terminating the test.

Somewhat better results were obtained with SiC-coated premelters. The coating generally prevented gross heater cracking although eventually during a test run some cracking would occur probably from silicon-graphite reactions at small pinholes in the coating.

Even without the cracking, another problem with the combination heater/crucibles was the tendency of the molten silicon to fill the slit forming the two electrode halves. The silicon surface tension was sufficient to hold it in the slit, creating an electrical short. This short would lower the current density near the heater tip, causing it to cool below the silicon melting point.

In view of the several problems encountered in using the various combination heater/crucible premelters, it was decided to insert fused silica "test tube" crucibles into the cylindrical heaters. This is the arrangement illustrated in Figure 2. Figure 6 is a photograph of the graphite heater showing the slit forming two electrodes. The 6-mm hole at the base of the slit was necessary to relieve stress during operation and prevent heater breakage. Figure 7 is a top view of the test tube premelter showing the attached copper electrodes and the fused quartz liner. A number of premelter insulation materials were tried including quartz, mullite, and alumina tubes slipped over the heater. Best results were obtained, in the end, by wrapping 6-mm thick graphite felt around the heater. The felt was held in place by thin molybdenum wire. The felt and wire had sufficiently higher electrical resistivity so that shorting of the heater was no problem. Overall electrical resistance of the heater was around 0.02 Ω. Figure 8 shows a power calibration curve of the graphite heater corrected for losses through the water-cooled electrodes.

Figure 6. Graphite Premelter Heating Element

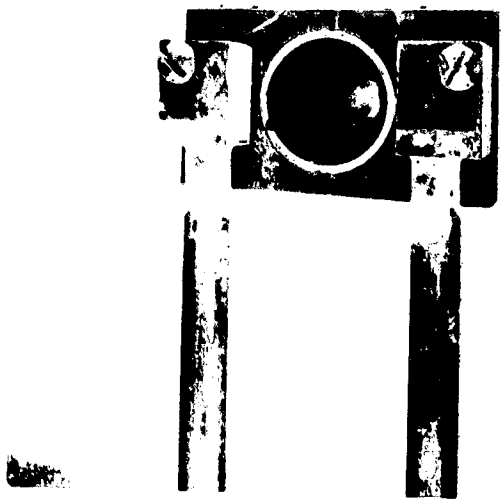

Figure 7. Top View of Premelter Showing Electrodes and Fused Quartz Liner

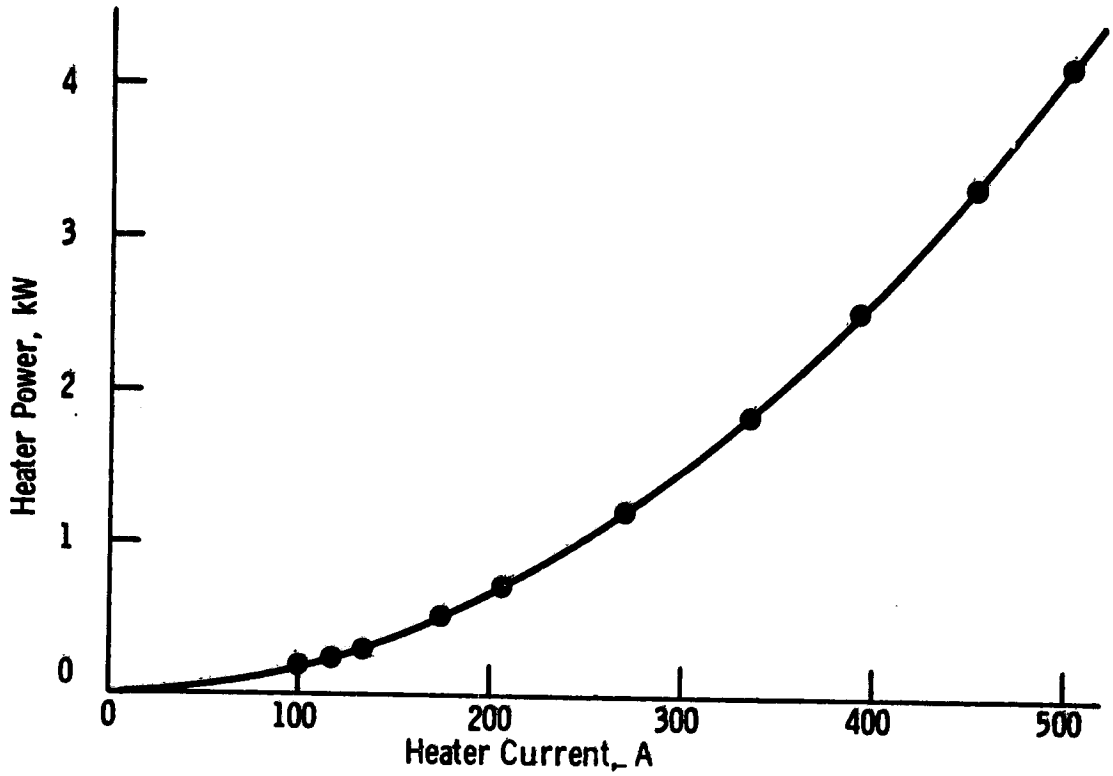

Figure 8. Test Tube Premelter Heater Power Calibration

Additional premelter discussion is provided in the section on puller test runs.

C. ADDITIONAL CONSIDERATIONS

1. Continuous Czochralski Doping

The crystal resistivity during continuous growth can be held constant by assuring that the incoming dopant flow contained in the polysilicon exactly equals the rate of incorporation into the crystal. A general dopant analysis along the lines indicated in reference 5 gives for the resistivity:

$$\rho/\rho_i = \frac{kC_{li}}{C_r - (C_r - kC_{li}) \exp(-kV_s/V_o)} \qquad (2)$$

where

C_{li} = initial melt dopant concentration

C_r = incoming melt replenishment concentration

V_s = crystal volume grown

V_o = primary crucible melt volume

k = dopant segregation coefficient

ρ_i = initial crystal resistivity, $V_s = o$

Equation (2) indicates that, without special precaution, the crystal resistivity will continually decrease as more crystal is grown due to the exponential term in the denominator. However, if $C_F = k C_{li}$, the exponential term drops out and the resistivity will remain constant, independent of crystal volume, V_S, grown. Thus, the incoming feed stream should be doped to a level $k C_{li}$ in order to maintain constant axial crystal resistivity profiles.

The last crystal grown in a continuous run will, of course, be grown without melt addition and its resistivity will obey the batch charge relation:

$$\rho/\rho_i = (1 - g)^{1 - k} \tag{3}$$

in which g is the fraction of melt solidified. To ensure a high resistivity yield, the crystal specification should be broad enough to encompass this last crystal resistivity variation. For boron dopant with k = 0.8 and at a grow yield of g = 0.9, the bottom of the last crystal will have a resistivity 0.63 that of the other crystals in the run.

2. Continuous Czochralski Impurity Buildup

Semiconductor-grade polysilicon contains trace amounts of various impurities such as iron, nickel, chromium, etc. These trace impurities do not normally present a problem for routine crystal growth. Solar-grade polysilicon at $10/kg is likely to contain significantly larger amounts of metallic impurities than current semiconductor silicon. Consequently, impurity buildup in continuous Cz could become a factor inhibiting crystal quality and grow yields.

Segregation coefficients of the trace metals range from 2×10^{-3} for aluminum[6] to around 4×10^{-6} for titanium and vanadium.[5] The melt impurity buildup in a continuous Cz process for materials having low k's was derived in reference 5 and is given, in slightly altered form, by:

$$C/C_O = 1 + G \tag{4}$$

where

C = melt (or solid) impurity concentration

C_O = initial melt (or solid) concentration

G = ratio of total crystal weight, W_c, pulled to initial melt weight, W_O. Same as the usual g in a batch pull.

Equation (4) is accurate within 5% for values of $kG \leq 0.1$. The buildup given by eq. (4) holds up to the last crystal which is then governed by the usual batch pull relation for small k:

$$C/C_O' = (1 - g)^{k - 1} \tag{5}$$

where C_O' is the melt impurity concentration at termination of silicon addition.

To illustrate, assume a baseline 100-kg process consisting of five 20-kg crystals with 1-kg tapers and a 1-kg button. Assume also that the primary crucible is a nominal 20-kg or 12-inch crucible. Then, at termination of melt addition, 2 kg into the fifth crystal, $G = 86/20 = 4.3$ and $C/C_0 = 1 + 4.3 = 5.3$ from eq. (4). At that point, eq. (5) governs and the final impurity concentration at start of taper as the fifth crystal is given by $C/C_0 = 5.3\,(1 - 0.9)^{-1} = 53$. The impurity buildup as a function of G for this assumed case is shown by the solid line in Figure 9.

An interesting alternate Czochralski strategy is that of pulling several crystals from a single large charge-multipulling. Impurity buildup in this case is simply the batch pull relation eq. (5). To achieve the same net crystal output as the continuous example above, the initial charge size would be 106 kg. At the end of the fifth 20-kg crystal, at start of taper, $g = 104/106 = 0.981$. This value of g in eq. (5) gives a final $C/C_0 = (1 - 0.981)^{-1} = 53$, precisely the same final result as in the continuous case. The multipull impurity buildup is shown by the dashed line in Figure 9.

Impurity buildup of a multicharge strategy could be examined using eq. (5) with results similar to those in Figure 2 of reference 5. The end result is exactly the same, i.e., the last crystal at start of taper would have a $C/C_0 = 53$. A major difference exists, however, between multicharging and the other two approaches in that each multicharge crystal in the run will exhibit impurity levels greater than those of the first four crystals in multipull or continuous runs. The majority of the impurities is confined to the last crystal in continuous and multipull whereas in multicharging they are distributed throughout all the crystals.

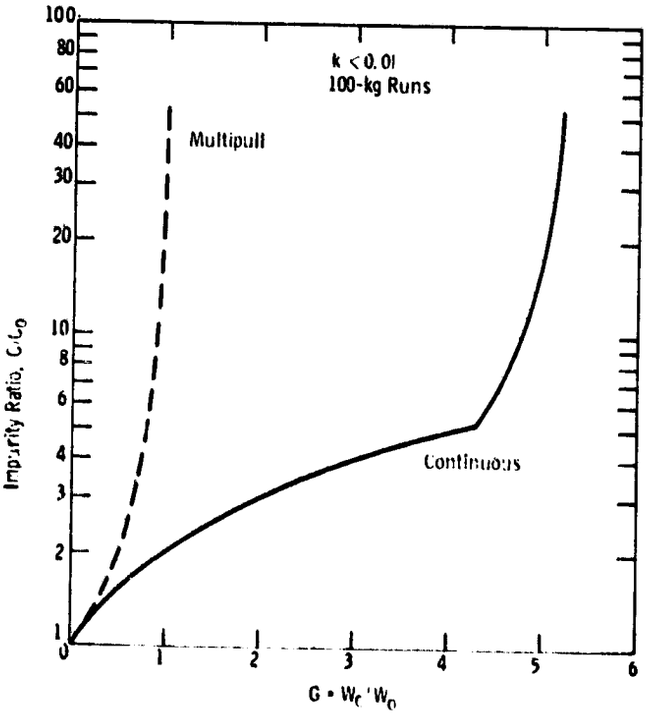

Figure 9. Impurity Buildup for Two Czochralski Strategies

The above observations imply that multicharging is a riskier strategy than continuous/multipull if solar-grade polysilicon is significantly dirtier than current semiconductor silicon. This implies, in turn, that the last crystal in a continuous run could be unusable due to excessive impurities or poor crystallinity.

3. Crystal Pull Rate

The crystal growth model developed in reference 4 was utilized to model 10-cm growth. Figure 10 shows theoretical maximum pull rates for continuous versus single-charge pulls from 12-kg crucible melts. At the longer crystal lengths, continuous growth provides a 25% pull rate advantage over batch growth. The indicated 19 cm/h continuous pull rate offers a comfortable margin over the 10 cm/h goal of the Czochralski programs.

4. Thermal Modeling

Early in this program, a model of the Varian 2848A hot zone assembly was developed to explore possible improvements in conjunction with the new lower dome fabrication. Results of this work were rather uninteresting in that no obvious changes were indicated which would dramatically improve hot zone control, response, or stability. Consequently, the standard 10-inch hot zone package was utilized in the experimental work.

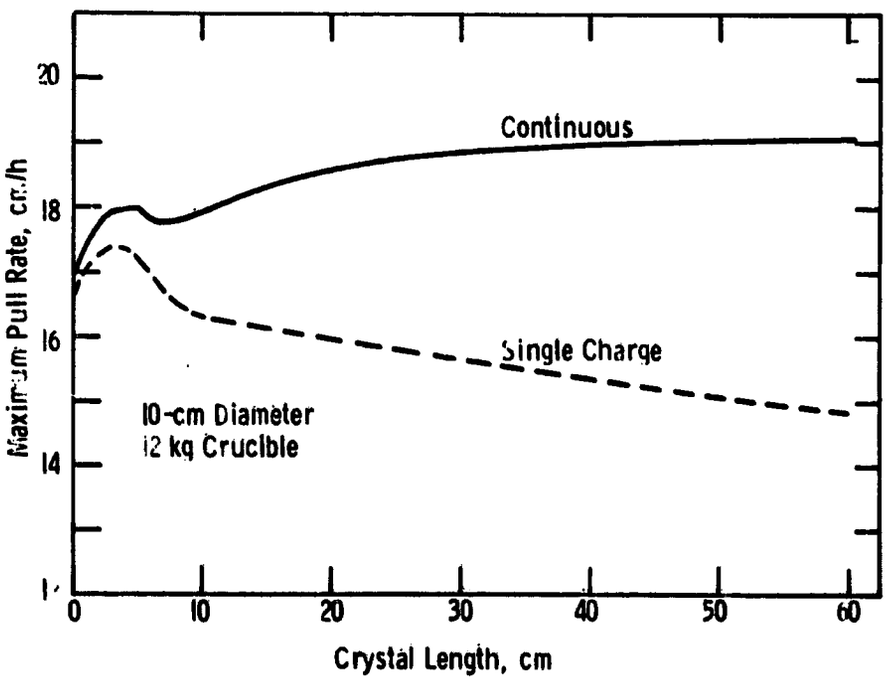

Figure 10. Theoretical Maximum Pull Rates of Continuous Versus Single Charge Czochralski Silicon Crystal Growth

A thermal model of the melt/crucible/crystal was developed to examine heat losses from these elements as a function of various parameters such as operational mode, crucible size and crystal size. Figure 11 compares heat losses to the furnace ambient for batch pull versus continuous crystal pulling. That figure assumes a nominal 10-inch crucible liner from which a 10-cm diameter crystal is growing. In the batch charge mode, heat losses from the melt and crucible continually increase as the crystal grows which means that furnace power must increase proportionally to maintain thermal equilibrium. On the other hand, continuous growth offers a fairly stable heat load to the furnace which means that temperature control of the melt would be more easily attained in this case.

Figure 12 illustrates the influence of crucible size on heat losses from the melt and crucible for continuous growth. A band is obtained because of the variation of the losses with crystal length. For instance, a 10-cm crystal growing from a nominal 10-inch liner (24.5 cm ID) will produce a heat loss varying from 8.5 to 10.2 kW as can be verified from Figure 11. Figure 12 suggests that there is a practical upper limit on crucible diameter and 35 cm (14 inches) may be approaching that limit. At this and larger diameters, heat shielding will be necessary to keep heat losses to a manageable level.

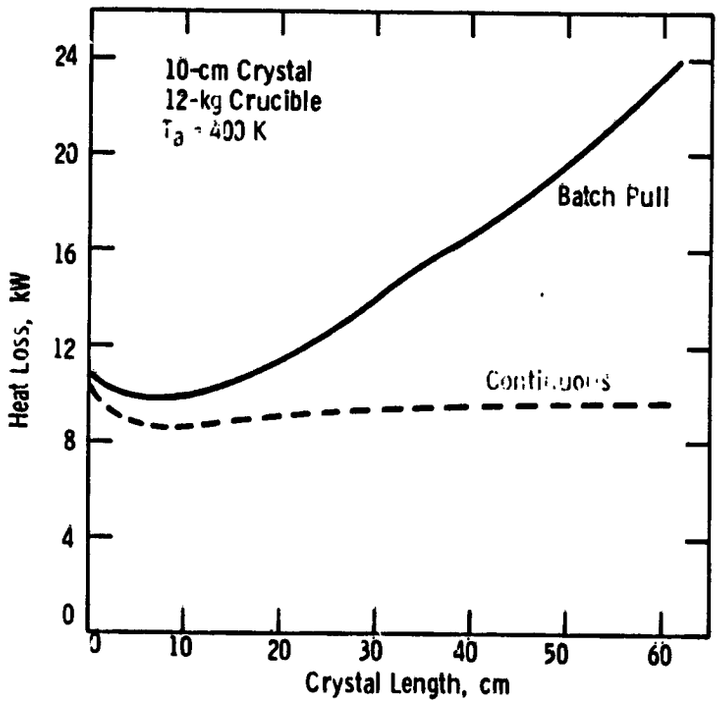

Figure 11. Combined Melt/Crucible Heat Losses During Crystal Growth

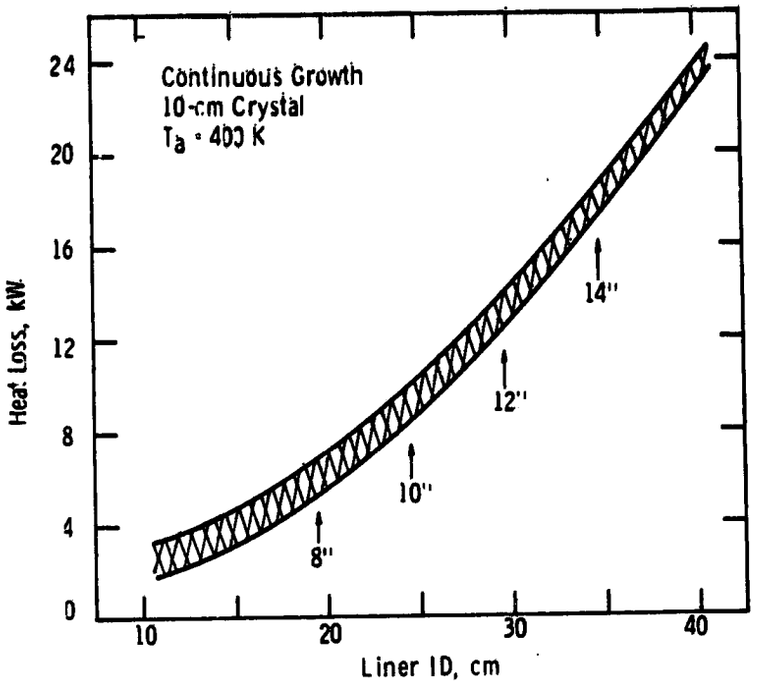

Figure 12. Combined Melt/Crucible Heat Losses as a Function of Crucible Size

D. TEST RESULTS

After assembly of the continuous puller, a number of batch pull runs were made to check out furnace operation and debug the puller. Approximately 1½ months were spent in this checkout phase in which controls were calibrated, leaks discovered and repaired, plumbing connections altered, and crystal growth experience gained. Eventually the puller operated satisfactorily as evidenced by good 7.6-cm diameter growth. At this point, premelter runs were started.

As was mentioned earlier, the Figure 1 premelter concept was abandoned in favor of the arrangement shown in Figure 13. The vertical orientation was the least preferred since it meant that 10-cm crystal could not be grown in the 12-kg crucible due to the physical space occupied by the premelter. To circumvent this problem, the premelter was tried initially angled over the crucible at a 60-degree orientation with approximately 3 cm extending over the edge of the crucible. This arrangement did not work for two reasons: (1) the molten silicon created severe melt vibration from dropping into the crucible from the excessive height, and (2) there was a tendency for the silicon fines to hang up in the premelter forming a bridge and preventing further entry of silicon.

Even in the vertical position, silicon bridging was fairly common initially and is illustrated in Figure 14. The graphite premelter heater is hottest at its tip and coolest at the top where the water-cooled electrodes are attached. Thus, there is a temperature gradient along its length and if the premelter were filled to a level near the cooler top, the silicon at the top would not melt.

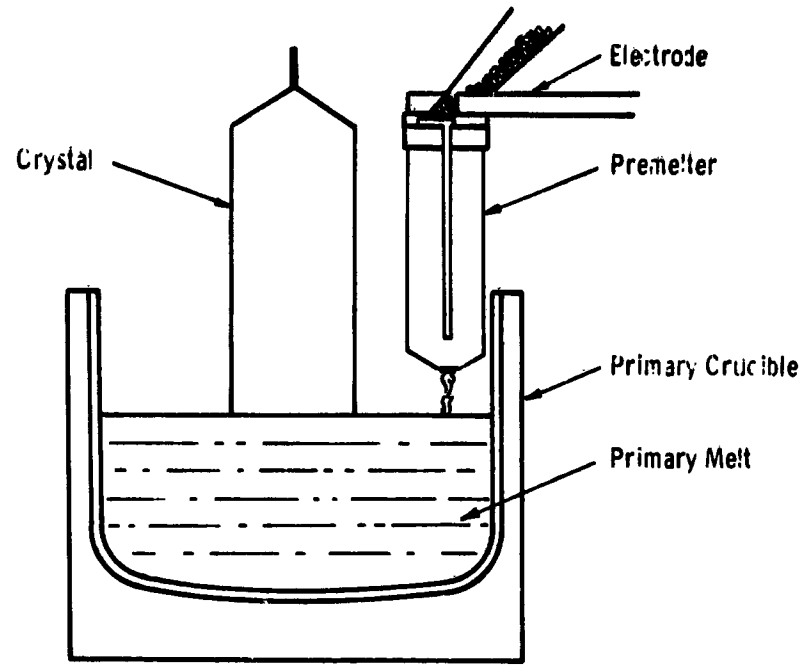

Figure 13. Test Tube Premelter in Position

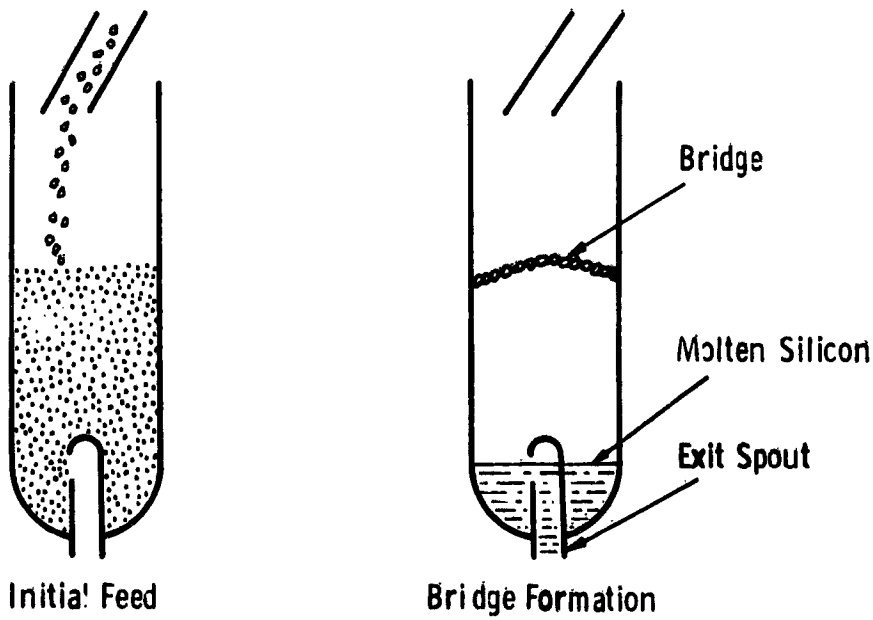

Figure 14. Test Tube Premelter Bridging

Instead, the silicon fines would sinter forming a solid bridge preventing additional silicon entry. This bridge was typically one particle thick and created a reflective heat shield for the silicon under it causing that silicon to melt and run out of the premelter. Three things were necessary to overcome the bridging: (1) the premelter was lengthened about 2 cm to create a longer, hotter region, (2) graphite felt insulation was necessary to minimize heat losses, and (3) the premelter was powered to operating conditions before any silicon was added which caused the silicon feed to melt virtually instantaneously as it entered the premelter.

The vertical test tube premelter will not provide a steady stream of molten silicon into the primary crucible. Instead, the silicon exits the premelter in discrete droplets or globules due to the surface tension holding molten silicon in the exit tube. Figure 15 shows the molten silicon head or height necessary to overcome surface tension as a function of the exit tube diameter. The premelters tested in this program had 6-mm diameter exit spouts. Thus, from Figure 15, a 2-cm head is required to cause flow from the exit tube. In operation, the premelter fills with molten silicon until a depth of this magnitude is achieved. At that point, the molten globule will rush out due to momentum until the liquid level is equal to the spout entry (refer to Figure 14). The fill process then repeats, resulting in discrete slugs of liquid silicon falling into the primary crucible.

If the premelter were positioned too far above the crucible, some splashing of molten silicon could be observed. To prevent splashing, one run was made with a fused quartz splash guard attached to the premelter. This guard was positioned so that approximately 2 mm was submerged

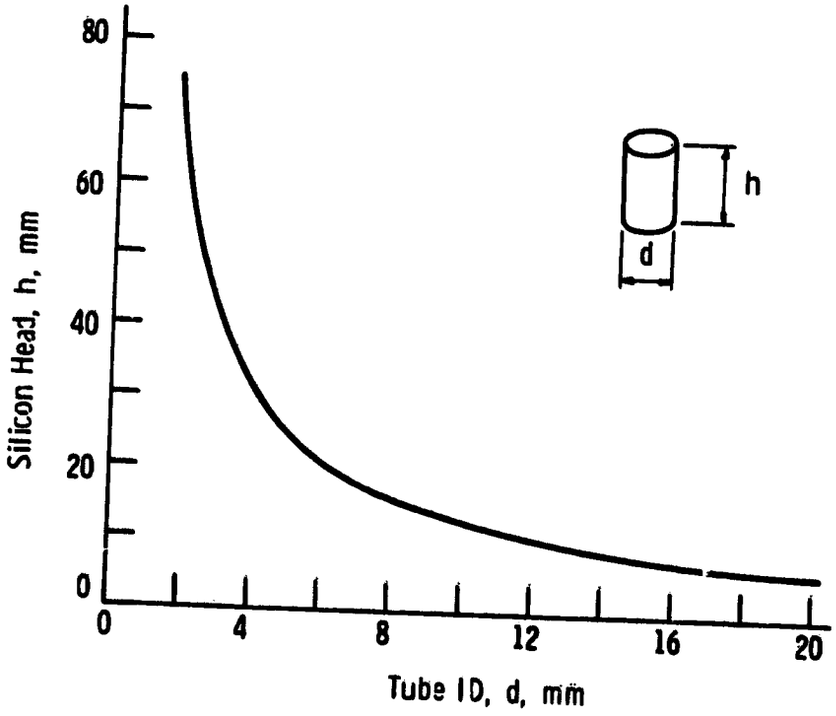

Figure 15. Silicon Head Required to Overcome Surface Tension

below the crucible melt surface. The splash guard created such severe thermal asymmetry that it was not possible to grow a crystal from the melt. Also, the guard did not prevent splashing nor did it damp out vibrations in the melt. It was abandoned after this one test in favor of simply raising the crucible until the melt level was only 2 mm or so from the premelter exit. This close positioning eliminated melt splashing and minimized agitation.

Four different heat shielding materials for the premelter were tried. First, clear fused quartz tubing was slipped over the graphite heater and suspended from the top electrodes with molybdenum wire. This shielding technique was abandoned because the quartz was simply not an effective radiation shield and it tended to react with the graphite, causing severe oxide buildup on the preheater. Similar tube shields were fabricated from alumina and mullite tubes and these worked considerably better than the quartz. However, ultimately ordinary 6-mm thick graphite felt was used which provided the best insulation properties. One layer of felt was wrapped around the heater and secured with small molybdenum wire. In addition to superior thermal insulation, the felt minimized the size of the premelter. Figure 16 is a photograph of a felt-insulated premelter.

Midway through the testing program, it was decided to replace the auger feed with a vibratory feeder. The auger O-ring seals were susceptible to fine silicon dust working its way into them, scoring the shaft, and causing leaks. The seals were reworked once successfully but when it was apparent they required a second reworking, it was decided to go to a Syntron-type bin feeder

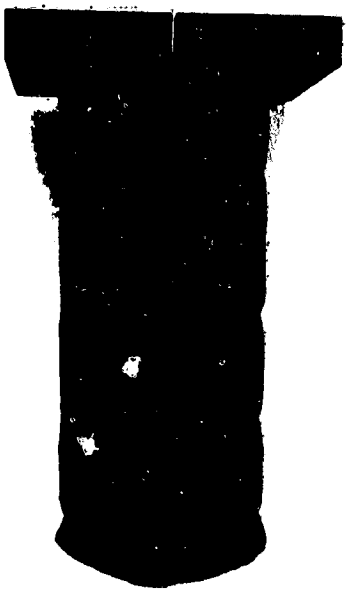

Figure 16. Premelter with Graphite Felt Insulation

enclosed in a vacuum-tight chamber. This unit fed granular silicon fines to the premelter through a 12-mm ID Teflon tube and worked reasonably well. Occasionally the silicon would block the line but light tapping on the Teflon would dislodge the blockage. This blockage was puzzling until it was realized that friction between the silicon granules and the tube created an electrostatic charge on the silicon causing it to stick to the side of the Teflon. Once a few silicon granules stuck, they would then create a dam behind which the incoming flow would back up, creating a blockage. This can be prevented by using a grounded metal inlet tube.

The procedure on the experimental runs was to melt 5 or 6 kg of ordinary chunk polysilicon in the primary crucible and raise the crucible until the melt level was within 2 mm or so of the premelter exit spout. Premelter power was turned on prior to seed and top growth so that thermal stability could be achieved. Once top growth was completed and a few centimeters of crystal were grown, polysilicon feed to the premelter could be started. Crystal growth would then proceed with melt addition until the run was terminated.

On a few occasions, the premelter was turned on after the crystal top had been rolled. Every time this was tried the sudden thermal shock would cause the crystal to cut in and lose perfection. For good top growth, it is absolutely essential that thermal equilibrium be established prior to seed-in which means that the premelter needs to be at or near operating temperature from the very beginning before seed-in is started.

Twenty-nine experimental runs were made with test tube premelters but only eight runs could be considered reasonably successful. In those eight runs, 83 cm of nominal 6-cm diameter crystal was grown with melt addition during growth. The best run achieved 21 cm of growth with melt addition. However, all the crystal grown with melt addition was high-dislocation primarily due to oxide problems. The unsuccessful runs failed for every reason known to Czochralski crystal growth: puller leaks, crucible shaft vibration, furnace and premelter power supply malfunctions, premelter electrode breakage, electrical arcing, vacuum pump failure, etc.

The number one problem encountered in the continuous growth runs was oxide buildup. Six sources were identified as potential oxide contributors: (1) puller leaks, (2) oxide evaporation from the primary melt surface, (3) water leaks, (4) surface oxide from the granular silicon feed, (5) premelter fused quartz liner-graphite reaction, and (6) fused quartz heat shield-graphite reaction. Whatever the oxide source, it will collect on any relatively cool surface and the premelter water-cooled electrodes were very convenient in this regard. Also, the SiO and SiO_2 would collect all along the outside of the premelter with a continual buildup as a run progressed. Eventually, a piece or, sometimes, a large chunk would drop off into the crucible invariably attaching to the growing crystal thereby ruining its crystallinity.

All the oxide sources listed above were systematically investigated but it was impossible to eliminate that from the primary melt and that from the premelter granular silicon. Consequently, it is doubtful that the test tube premelter approach pursued in this program can result in 100-kg runs of dislocation-free single crystal. Interestingly, melt agitation caused by the liquid addition in these runs did not seem to adversely affect crystal perfection. The key is to minimize melt agitation by keeping the melt level either adjacent to the premelter exit or submerge the exit spout. This

latter item was attempted once but the crucible was raised too far and contacted the graphite premelter heater. This caused the heater to break as it reacted with the molten silicon to form SiC. No further attempts were made to submerge the exit spout.

Only two crystals were characterized for oxygen and carbon due to a lack of sufficiently interesting product to justify the expense and trouble. A 7.6-cm boron-doped crystal grown in batch mode to check puller operations is presented in Table 2. The C and O levels in Table 2 are quite normal.

Table 2. Batch Pull Carbon and Oxygen

g	Oxygen	Carbon
0.02	1.6×10^{18} a/cm^3	Nondetectable
0.79	1.3×10^{18}	7.4×10^{16}

One crystal grown with continuous feed was measured and the results are shown in Table 3. Crystal diameter was 5 cm and it was undoped. Melt addition began 3.2 cm down from the top roll and ended 17.2 cm down. Total length of the 5.0-cm diameter crystal was 21.1 cm. Oxygen looks a little low and the carbon is a little high, which could be due to the influence of the graphite premelter heater although too much should not be inferred from one set of measurements.

Table 3. Continuous Pull Carbon and Oxygen

Location	Oxygen	Carbon
Top roll	1.2×10^{18} a/cm^3	5.3×10^{16} a/cm^3
3.2 cm after feed started	1.0×10^{18}	8.2×10^{16}
5.8 cm after feed started	1.2×10^{18}	9.3×10^{16}
Bottom, no feed	1.0×10^{18}	13.5×10^{16}

E. ECONOMIC MODELING

The IPEG option of SAMICS[1] was used to estimate costs of the continuous Czochralski process described. Fairly conservative assumptions were made regarding labor, supplies costs, and yields. A 100-kg furnace run results in 545 cm of 10-cm diameter crystals. For a baseline process, it is assumed that five crystals, each of 109-cm length, will be grown in one run for a total of 545-cm crystal at 100% yield. A summary of the basic model assumptions is given below with backup information in Appendix B.

1. Basic Assumptions

a. 100-kg Furnace run

b. 10-cm Diameter crystal pulled at 10 cm/h

c. Equipment cost is $130,000

d. Equipment utilization is 83%

e. Furnace floor space is 150 ft^2

f. Run cycle time is 72.0 h

g. Two pullers per operator

h. Direct labor cost $5/h

i. Operating supplies are $538/furnace run

j. Power per run is 4180 kW-h at $0.03/kW-h

k. 100% Yield/run is 101.66 m^2 in slice equivalent area based on 25 slices/cm crystal at 95% saw yield.

The above cost assumptions are in 1978 dollars. Later these costs will be adjusted back to 1975 dollars per the IPEG inflation factors in order to remain compatible with the 1982 cost goals.

2. IPEG Inputs

a. Furnace Runs/Year

With the assumed 83% utilization factor applied to a 24-h day, 364-day year the furnace runs/year are:

$$\text{Runs/year} = (0.83)\,(24)\,(364)/72.0 = 100.7$$

b. Direct Labor

$$\text{Labor/run} = (72.0\text{ h})\,(\$5.00/\text{h})/2 = \$180.00$$

$$\text{Direct labor/year} = (\$180.00)\,(100.7) = \$18{,}127$$

c. Operating Materials

From Appendix B the materials costs/run are $538.00. The annual materials costs are:

$$\text{MATS} = (\$538.00)\,(100.7) = \$54{,}177$$

d. Utilities

The only utilities cost of consequence is the electrical power per run assumed at $0.03/kW-h.

$$\text{Cost/run} = (4180 \text{ kW-H})(\$0.03) = \$125.40$$

$$\text{Utilities/year} = (125.40)(100.7) = \$12,628$$

e. Crystal Output

At 100% crystal yield, 545 cm crystal will be produced, which, at 23.75 slices/cm yields 101.66 m^2 per furnace run. Then,

$$\text{QUAN} = (101.66)(100.7) = 10237.16 \text{ m}^2/\text{yr}$$

3. IPEG Cost

The IPEG cost model uses the equation:

$$\text{Cost} = (0.49 \cdot \text{EQPT} + 97 \cdot \text{SQFT} + 2.1 \cdot \text{DLAB} + 1.3 \cdot \text{MATS} + 1.3 \cdot \text{UTIL})/\text{QUAN}$$

where

EQPT = equipment cost = $130,000

SQFT = space requirements per furnace = 150 ft^2

DLAB = annual direct labor = $18,127

MATS = annual materials cost = $54,177

UTIL = annual utilities cost = $12,628

QUAN = annual output = 10237.16 m^2

With these parameters, the IPEG cost is $19.85/$m^2$. Deflating this cost back to 1975 dollars using a 1.275 inflation factor, gives a 1975 equivalent cost of $15.57/$m^2$ at 100% crystal yield.

4. Total Crystal Cost

Polysilicon expense can be added easily to the above crystal processing cost using 10o kg/run and the same slice equivalent area. Total crystal costs in 1975 dollars are shown in the table below for unburdened polysilicon.

Poly Cost	1975 Crystal Cost – 100% Yield
$ 0/kg	$15.57/m^2
10	26.00
25	41.64
60	78.13

Figure 17 shows the above crystal costs as a function of yield. On a grams in-grams out basis, a crystal yield of 80% or better should be feasible in a continuous process.

5. Total Wafer Cost

Crystal slicing costs must be added to the above to arrive at the final slice value. Varian[7] has projected sawing costs in the 1984 time frame at $20.23/m^2 in 1975 dollars. This sawing cost is independent of crystal yield and will add directly to the costs shown in Figure 17. For example, crystal grown from $25/kg polysilicon with an 80% yield will result in a slice cost of $72.28/m^2 which is comfortably below the JPL 1982 guideline[1] of $128/m^2.

The 1986 cost goal of $18.20/m^2 presents a considerably more formidable challenge. In fact, as the above table and Figure 17 indicate, this cost goal cannot be met unless polysilicon is free, crystal yield is 100%, and sawing costs are reduced to $2.63/m^2 if one adheres to the assumptions

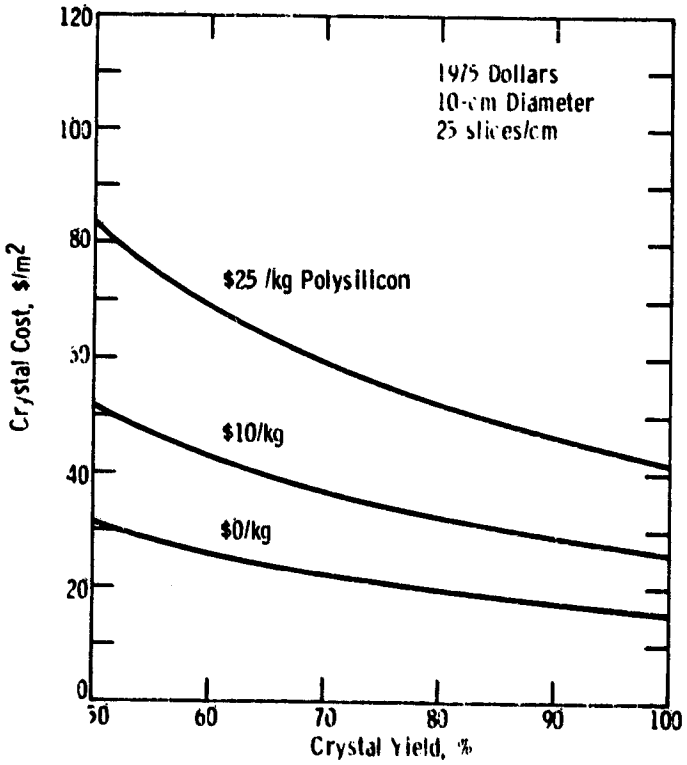

Figure 17. SAMICS/IPEG Continuous Czochralski Crystal Cost Expressed in Equivalent Slice Area

listed on page 24. This sawing cost would represent an additional order-of-magnitude reduction from an already optimistic slicing cost projection[7] and is unattainable. Consequently, one is forced to conclude that Czochralski silicon cannot meet the 1986 wafer cost goal. Nevertheless, Czochralski can meet the intermediate and near-term cost goals and is worth pursuing on that basis alone.

6. Cost Sensitivity

The sensitivity of crystal cost to run size and crystal size were estimated using the previous cost assumptions. However, operating supplies costs were altered slightly. These supplies were assumed $338/run exclusive of argon and crystal seeds up to the 100-kg run level. For runs larger than 100 kg, supplies were increased 1% per kilogram per run. Thus, a 120-kg run would consume ($338) (1.2) = $405.60 in operating supplies. In addition, argon costs, which are proportional to cycle time, were assumed $2.50/h (50 cfh X $0.05/ft^3) which corresponds with recent operating experience.

a. Furnace Run Size

The sensitivity of crystal cost to run size was examined assuming a crystal weight of 20 kg, exclusive of bottom taper. This crystal weight is convenient from a handling and length standpoint and is compatible with current practice. Table 4 gives pertinent data for this case along with the yearly costs used in IPEG.

A graph of the resulting crystal costs is shown in Figure 18. It is very interesting that the cost curves approach a minimum asymptote at about 100 kg/run. The reason for this is apparent from Table 4. Yearly labor cost per furnace is independent of the number of runs and materials, utilities, and wafer output are essentially constant from 100 kg up. Thus, crystal costs flatten out and become independent of run size. As mentioned, material costs were increased proportional to run size above 100 kg. However, removing this restriction does not alter the fundamental result. If materials were held constant at $338/run, crystal costs at the 200 kg/run level would be only 10% lower than those shown in Figure 18.

b. Crystal Size

The effect of crystal size on add-on costs was examined for nominal 100-kg runs. Table 5 presents pertinent parameters for this analysis and Figure 19 shows the results using IPEG.1 Crystal cost varies linearly with the number of crystals/run. Obviously, it would be foolish to grow 10 crystals in a 100-kg run but this case is shown in Table 5 and Figure 19 to give some indication of the cost penalty incurred in pulling plugs.

Note that polysilicon consumption increases with the number of crystals/run due to the additional silicon lost in the bottom tapers. Consequently, the total crystal cost including polysilicon increases at a slightly greater rate than the slopes shown in Figure 19.

Table 4. Cost Parameters for Various Run Sizes
Nominal 20-kg Crystals
10-cm Diameter

Run Size	Poly Charged	Cycle Time	Power	Runs/Yr.	Labor/Yr.	Matl's./Yr.	Utilities/Yr.	Output	Add-on Cost
20 kg	22 kg	17.9 h	934 kW-h	405.0	$18,127	$155,014	$11,348	8,234 m^2	$31.68/$m^2$
40	43	31.3	1738	231.6	18,127	97,562	12,076	9,417	21.56
60	64	44.7	2542	162.2	18,127	74,571	12,369	9,893	18.18
80	85	58.1	3346	124.8	18,127	62,182	12,527	10,149	16.49
100	106	72.0	4180	100.7	18,127	54,177	12,628	10,237	15.57
120	127	85.4	4984	84.9	18,127	54,684	12,694	10,357	15.44
160	169	112.2	6592	64.6	18,127	55,317	12,775	10,507	15.29
200	211	139.0	8200	52.1	18,127	55,669	12,817	10,592	15.21

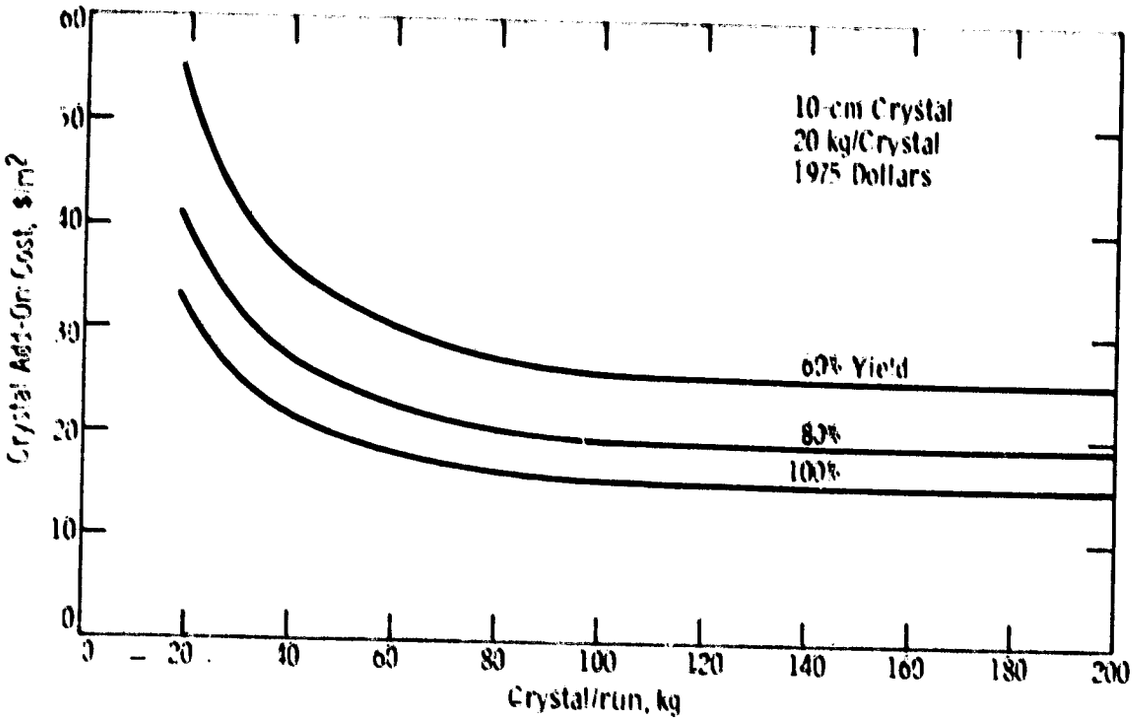

Figure 18. Effect of Furnace-Run Size on Continuous Czochralski Add-On Cost

7. Cost Discussion

Figure 20 shows a bar chart of the cost elements for the baseline continuous Czochralski process at the 1986 polysilicon goal of $10/kg. The crystal slicing costs are taken from reference 7. Crystal costs are based on an 80% yield which should be feasible in a continuous growth process. The baseline Cz process is that of five 20 kg crystals per furnace run grown from a 20-kg crucible.

The total Cz process cost exclusive of polysilicon is approximately $39 m^{-2} which is over twice the 1986 goal of $18.20/m^{2}. The implication is that continuous Cz cannot meet the 1986 wafer cost goal. This $39 m^{-2} add-on cost is almost equally split between crystal growth and sawing with no single cost element standing out as deserving of special attention. Consequently, attention to all cost elements is justified with crystal slicing just as important as crystal growth. It is emphasized that the $20.23 m^{-2} sawing cost used in Figure 20 represents a highly optimistic cost reduction from the current $70 m^{-2} cost.[7]

8. Alternate Strategies

Two alternate approaches for Cz crystal growth are suggested as having some merit: (1) larger diameter crystal, and (2) multipulling, which refers to growing several crystals from a single crucible without intermediate recharging. Larger diameter crystal offers an immediate productivity improvement since a continuous puller for 10-cm crystal probably could be scaled up to 12 or 12.5 cm with minimal difficulty. Although for constant slice thickness the wafer area per run is independent of diameter, 100 kg of the larger crystal could be grown in less time than 10 cm resulting in more furnace runs per year.

Table 5. Cost Parameters for Various Crystal Sizes
Nominal 100-kg Runs
10-cm Crystal

No. Crystals	Poly Charged	Cycle Time	Power	Runs/Yr.	Labor/Yr.	Matl's./Yr.	Utilities/Yr.	Output	Add-on Cost
4	105 kg	69.4 h	4024 kW-h	104.4	$18,127	$54,967	$12,663	10,593 m^2	$15.12/$m^2$
5	106	72.0	4180	100.7	18,127	54,177	12,628	10,237	15.57
6	107	74.4	4324	97.4	18,127	53,473	12,635	9,884	16.05
8	109	79.4	4624	91.3	18,127	52,178	12,665	9,265	16.98
10	111	84.4	4924	85.9	18,127	51,025	12,689	8,717	17.92

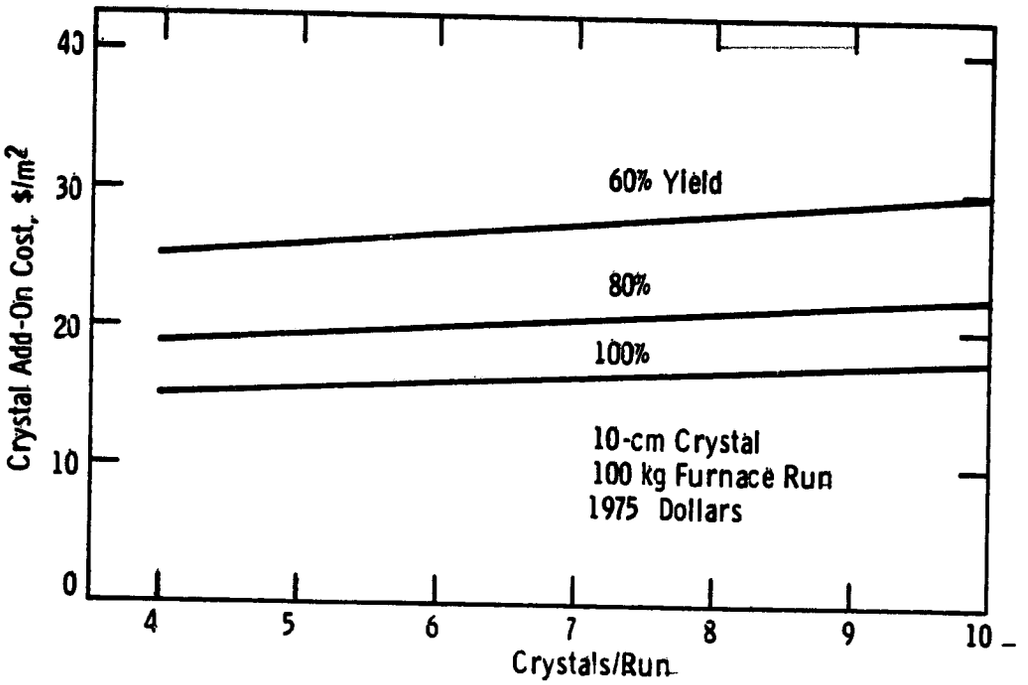

Figure 19. Effect of Crystal Size on Continuous Czochralski Add-On Cost

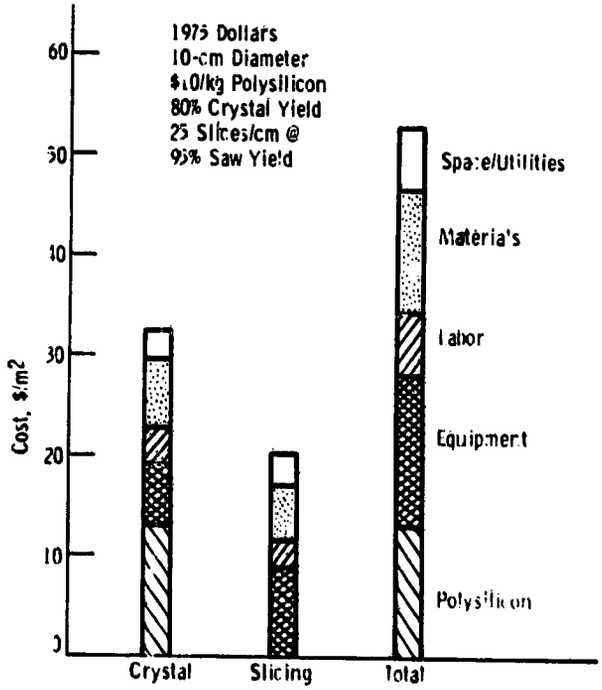

Figure 20. SAMICS/IPEG Cost Breakdown of a Continuous Czochralski Slice Process

Table 6 compares costs of both 12.5 cm and 15 cm crystal with the 10-cm baseline. The crystal costs in Table 6 are add-on costs at 100% yield in 1975 dollars. All assumptions built into Table 6 are the same as for the 10-cm baseline process. Thus, going to 12.5-cm crystal offers a 20% cost savings over 10-cm crystal. However, when polysilicon and sawing costs are added in, the net savings in total cost is only 8%.

Table 6. Crystal Diameter Impact on Cost
100-kg Continuous Runs

Crystal Dia.	Cycle Time	Runs/Yr.	Output/Yr.	Matl's./Yr.	Utilities/Yr.	Crystal Cost
10.0 cm	72.0 h	100.7	10,237 m^2	$54,177	$12,628	$15.57/$m^2$
12.5	52.3	138.6	14,068	67,741	12,715	12.32
15.0	41.7	173.9	17,651	80,385	12,636	10.54

A multipulling strategy is attractive in that it is a relatively straightforward extension of conventional batch pull Czochralski and, therefore, is lower risk than continuous Cz. Costs were estimated using previous assumptions with the exceptions:

1. Furnace cost: $120,000
2. Operating supplies: $262 plus argon at 60 scfh and $0.05/$ft^3$
3. Liner cost: $400
4. Labor cost: $12,085/year/furnace.

The liner cost is estimated based on a 40 X 34 cm (16" X 13.5") 100-kg liner. With this liner size, the net crystal per run is around 92 kg. Table 7 gives pertinent cost data for multipulling. Again, crystal costs listed in Table 7 are add-on at 100% yield in 1975 dollars. Although indicated crystal costs are higher for multipulling than for continuous growth, the simplicity of this approach could make the net cost differential in practice considerably less.

Table 7. Multipull Crystal Costs
100-kg Runs

Crystal Dia.	Cycle Time	Runs/Yr.	Output/Yr.	Matl's./Yr.	Utilities/Yr.	Crystal Cost
10.0 cm	71.0 h	102.1	9,522 m^2	$ 84,964	$16,033	$18.55/$m^2$
12.5	53.0	136.8	12,759	111,492	17,196	16.05
15.0	43.2	167.8	15,644	131,824	17,392	14.43

SECTION III
CONCLUSIONS AND RECOMMENDATIONS

The modest success demonstrated by this initial phase of continuous Czochralski process development was encouraging from an overall standpoint in that several areas of uncertainty were clarified and specific problems requiring additional investigation were identified. Major findings included:

1. A flow of granular silicon can be melted in a fairly simple, inexpensive premelter.
2. Overall power consumption of a continuous Cz furnace utilizing an in-situ premelter is the same as a batch charge furnace. The heated premelter acts as an insulator to the primary crucible so that its heat losses are reduced by approximately the premelter power input.
3. Vibratory feeders for metering solid silicon flow are preferred, at least for granular silicon.
4. The presence of a heated premelter adjacent to a growing crystal presents no particular problem as long as the premelter is maintained at operating temperature from start of crystal growth. The maximum crystal pull rate appears to be reduced somewhat, however.
5. Melt agitation from the incoming molten silicon droplets does not, of itself, destroy crystallinity. Melt agitation can be reduced by submerging the premelter exit spout below the primary crucible melt level. Excessive melt vibration is harmful because it dislodges particulates from the crucible sides which can then strike the growing crystal and destroy its perfection.
6. The VAT pneumatically operated and water-cooled vacuum valve operated flawlessly. Hot changes can be reduced to a fairly routine operation with the aid of this or similar valves. Few particulates were dropped into the melt by the valve operation.
7. Crystal diameter control is unaffected by the premelter and melt addition even for melt level fluctuations of ±10 mm. It was found that by calibrating the inlet silicon flow rate and matching this against the crystal growth conditions, the melt level could be held within this 10-mm tolerance without active melt level control.
8. From economic and operational standpoints, 100-kg furnace runs consisting of 4 or 5 crystals per run are optimal. A negligible cost improvement is obtained for larger runs.

Several items of a negative nature became apparent during the investigation.

9. Oxide buildup on the premelter was the major problem inhibiting more extensive continuous runs. There are at least six sources of oxide, most of which were encountered at one time or another: (a) melt-liner reaction, (b) puller leaks, (c) water leak inside the puller, (d) premelter quartz liner-silicon reaction, (e) oxide from the granular silicon surface, and (f) quartz heat shield-graphite reaction. This last source was eliminated by going to the graphite felt insulation. Mullite was found also to be quite effective as a thermal radiation shield with alumina and quartz, in that order, being of lesser effectiveness because of their contribution to the oxide problem.

   The oxide buildup on the premelter eventually grows to the point where a piece will flake off, fall into the melt, and ruin the crystal. On several instances, oxide formed across the mouth of the premelter liner, completely blocking entry of additional silicon. Both the silicon fines and the test tube liner are believed to be contributors to this phenomenon.

   No solution to the oxide problem is obvious. Any relatively cool surface extending over the primary melt offers a condensation area for the SiO and, occasionally, SiO_2. Several more experimental runs are necessary for a definitive conclusion to the care, feeding, and prevention of oxide buildup.

10. Auger feed mechanisms for silicon are not recommended. They do an excellent job of grinding silicon into smaller fines which then destroy shafts, seals, and vacuums.

11. The premelter should be somewhat larger than was used in this work in order to provide a larger melt volume and enable the premelter to operate at a lower temperature. Unfortunately, a larger premelter requires a larger primary crucible for 10-cm crystal to be grown comfortably. A 14-inch crucible should be adequate rather than the 10-inch crucible employed in the program.

12. Cost projections of continuous Czochralski wafer processes are not promising for meeting 1986 cost goals. Crystal growth costs appear headed down substantially but slicing costs are far too high and even optimistic projections show slicing alone to exceed the total allowable cost for the entire wafer process. It is recommended that alternate sawing approaches to multiblade slicing be examined expeditiously.

13. An interesting crystal fallback position for the intermediate term could be a multipull Cz process which is only slightly more expensive than a continuous process.

SECTION IV
NEW TECHNOLOGY

Two items were submitted as new technology during the course of this investigation:

1. The basic concept of a continuous furnace having an in-situ premelter with attendant silicon storage and feed mechanism.
2. The compact, inexpensive test tube-design premelter consisting of a graphite heater surrounding a fused quartz cylindrical liner.

SECTION V
REFERENCES

1. R. G. Chamberlain, *SAMICS Workbook – Version 1*, JPL Document 5101-15, 1977.

2. F. Schmid and C. P. Khattak, *Silicon Ingot Casting – Fixed Abrasive Slicing*, Quarterly Report, DOE/JPL 954373-79/8, January 1979.

3. R. G. Wolfson and C. B. Sibley, *Development of Advanced Methods for Continuous Czochralski Growth*, Quarterly Report, DOE/JPL 954884-77/4, January 1978.

4. S. N. Rea and P. S. Gleim, *Large Area Czochralski Silicon*, Final Report, ERDA/JPL 954475-77/4, April 1977.

5. R. H. Hopkins, et al., "Crystal Growth Considerations in the Use of Solar Grade Silicon", *J. Crystal Growth*, 42 (1977) 493-498.

6. W. R. Runyan, *Silicon Semiconductor Technology*, McGraw-Hill, 1965, 108.

7. S. C. Holden and J. R. Fleming, *Slicing of Silicon into Sheet Material*, Quarterly Report, DOE/JPL 954374-78/1, April 1978.

36

APPENDIX A

ENGINEERING DRAWINGS

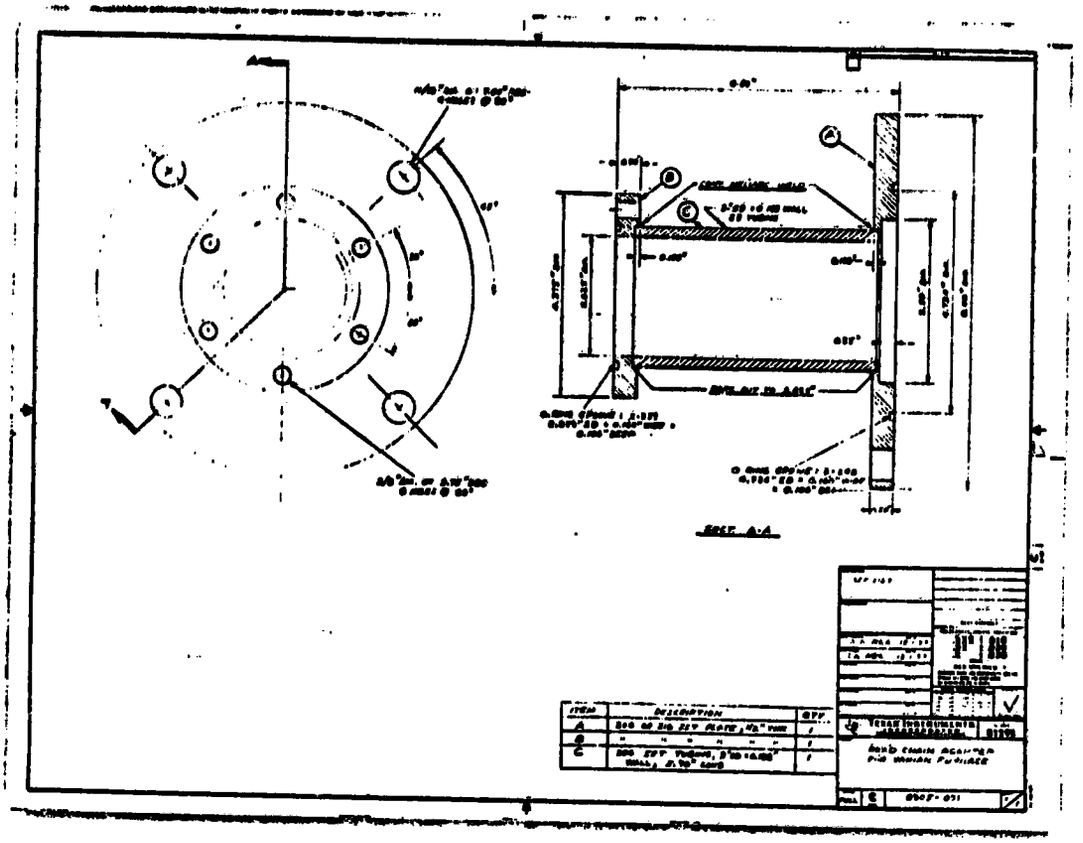

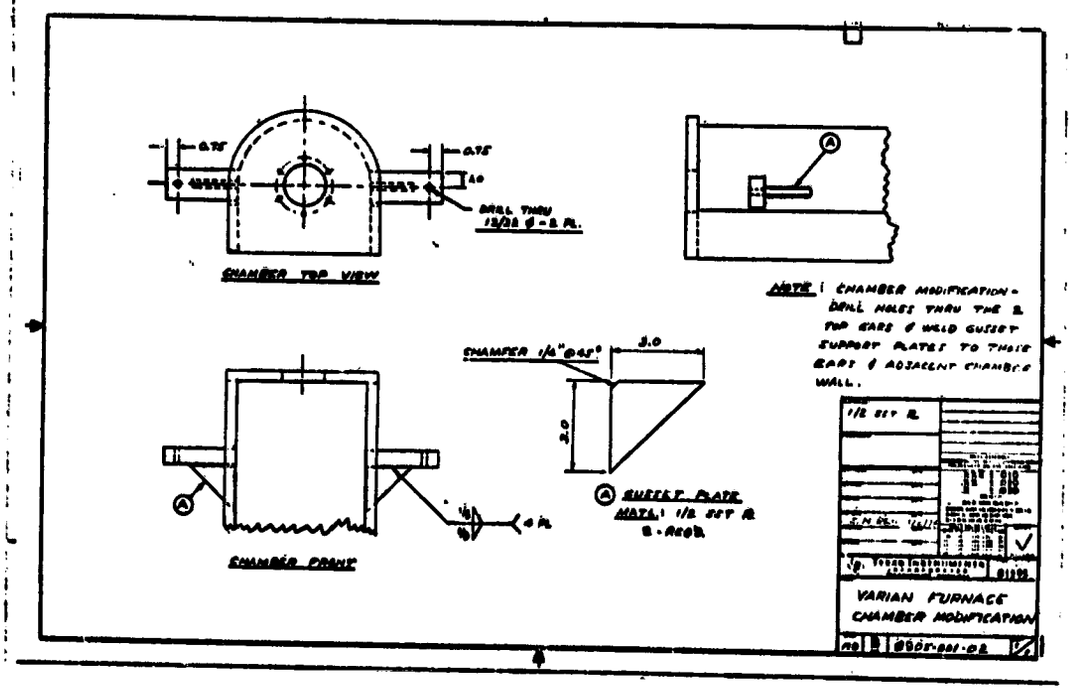

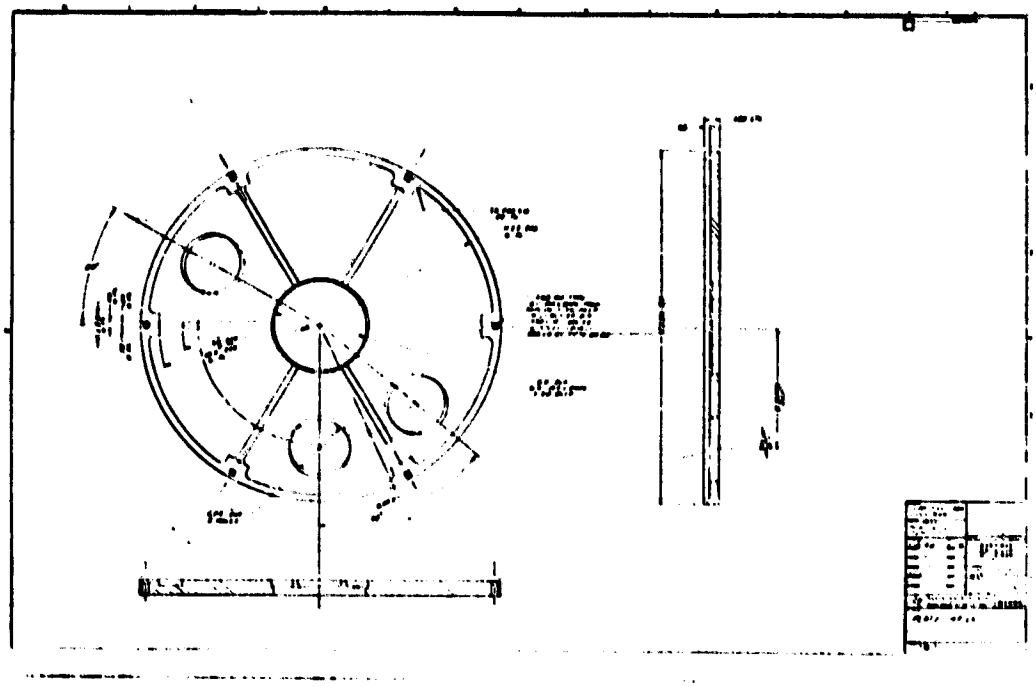

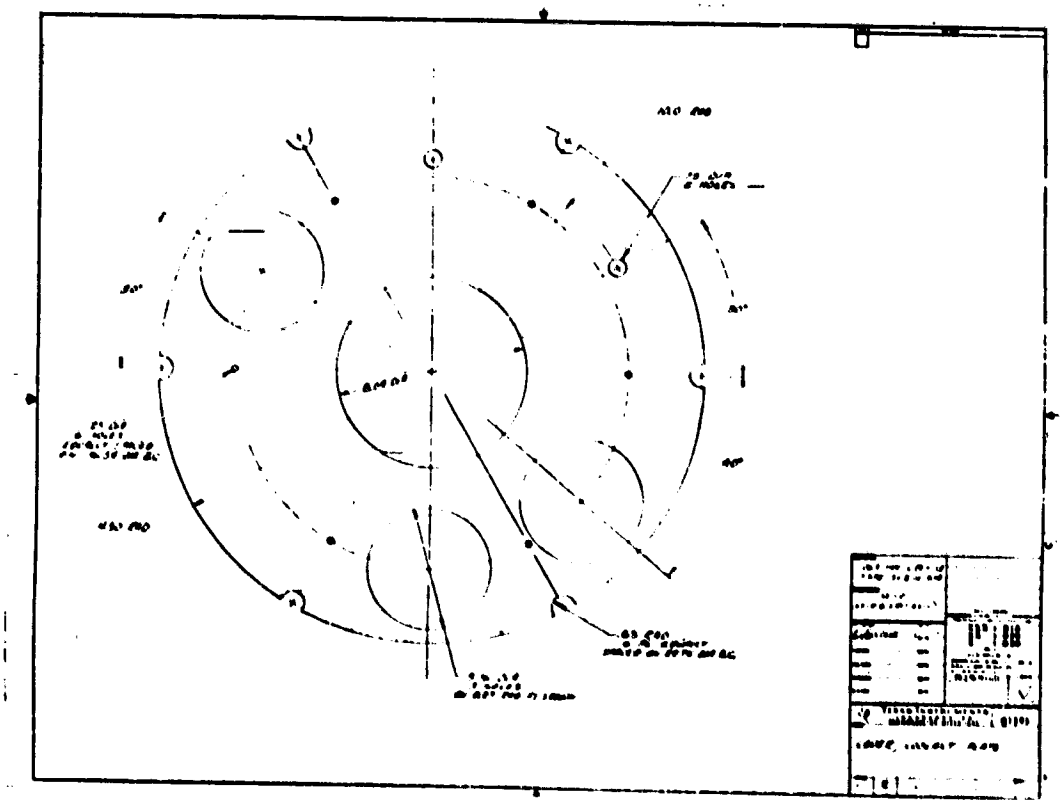

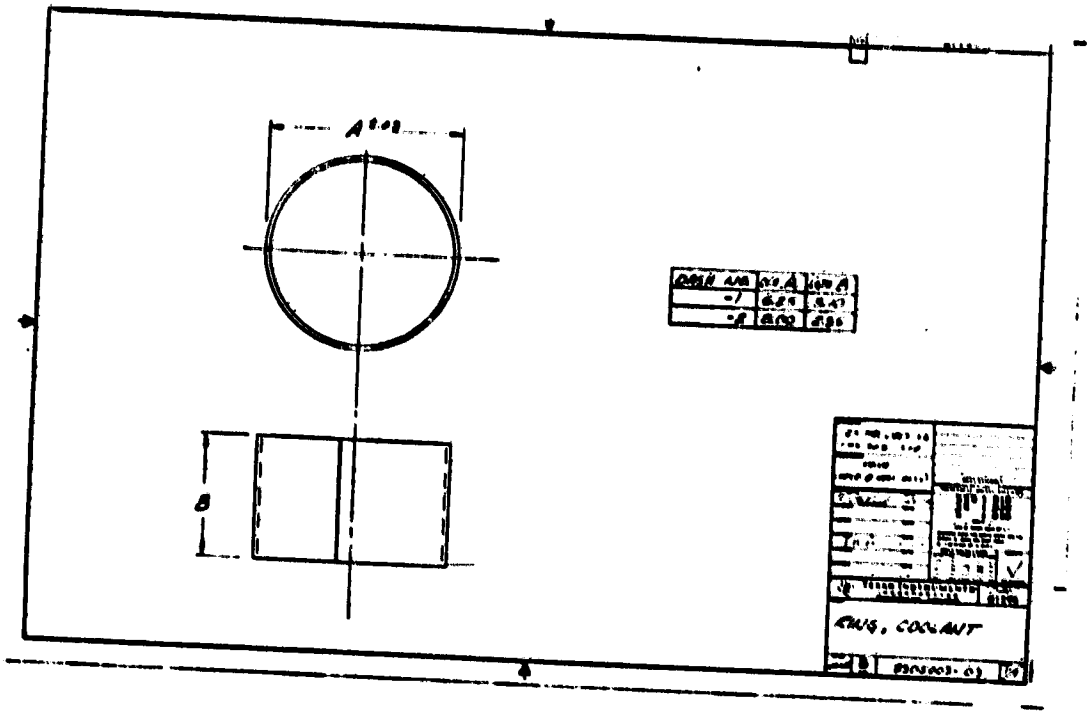
A
B
ENG. COOLANT

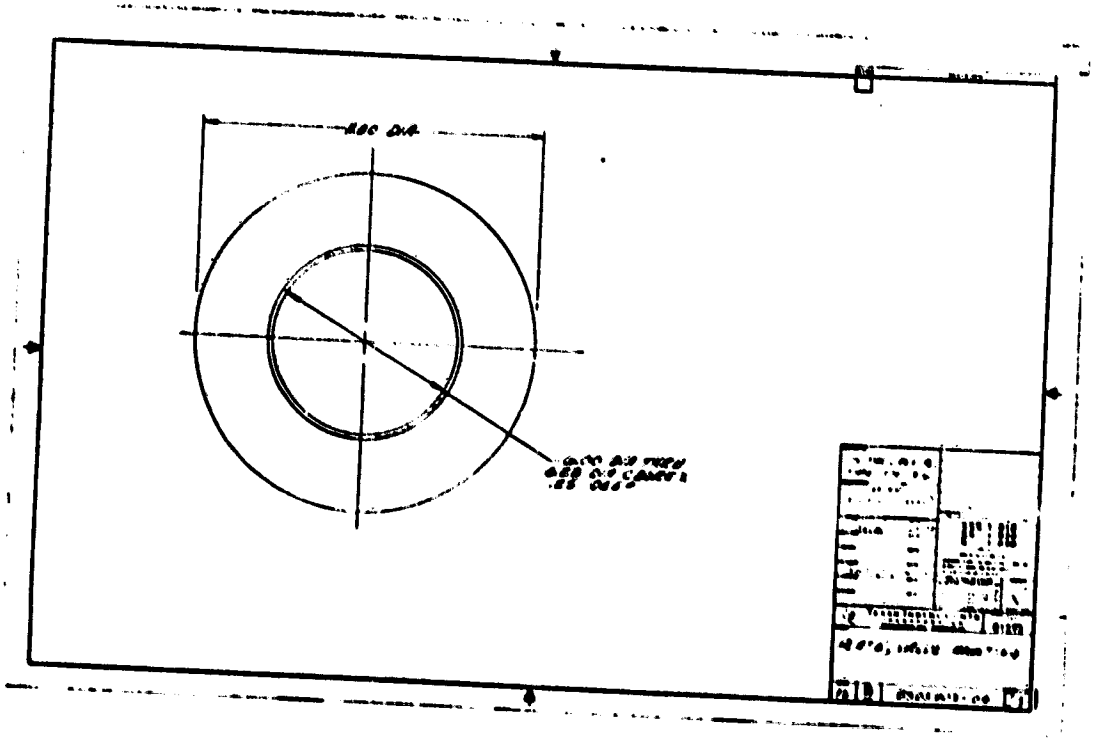

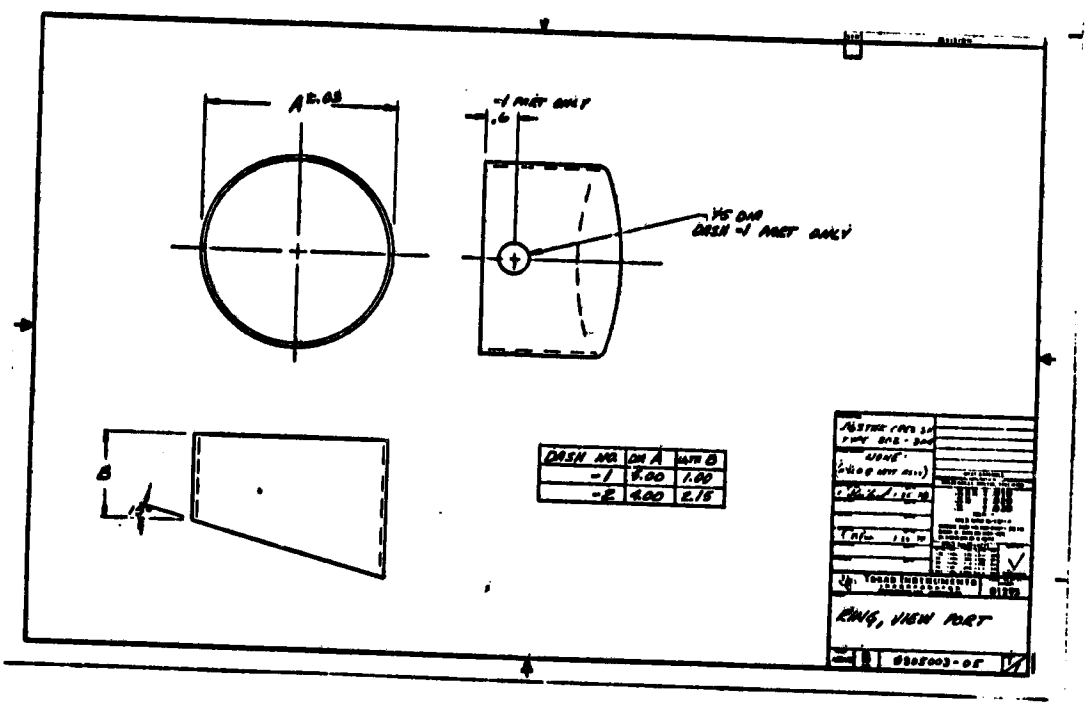
A ±.05
-1 PART ONLY
.6
.75 DIA
DASH -1 PART ONLY
B
DASH NO. | DIM A | DIM B
-1 | 3.00 | 1.00
-2 | 4.00 | 2.75
RING, VIEW PORT

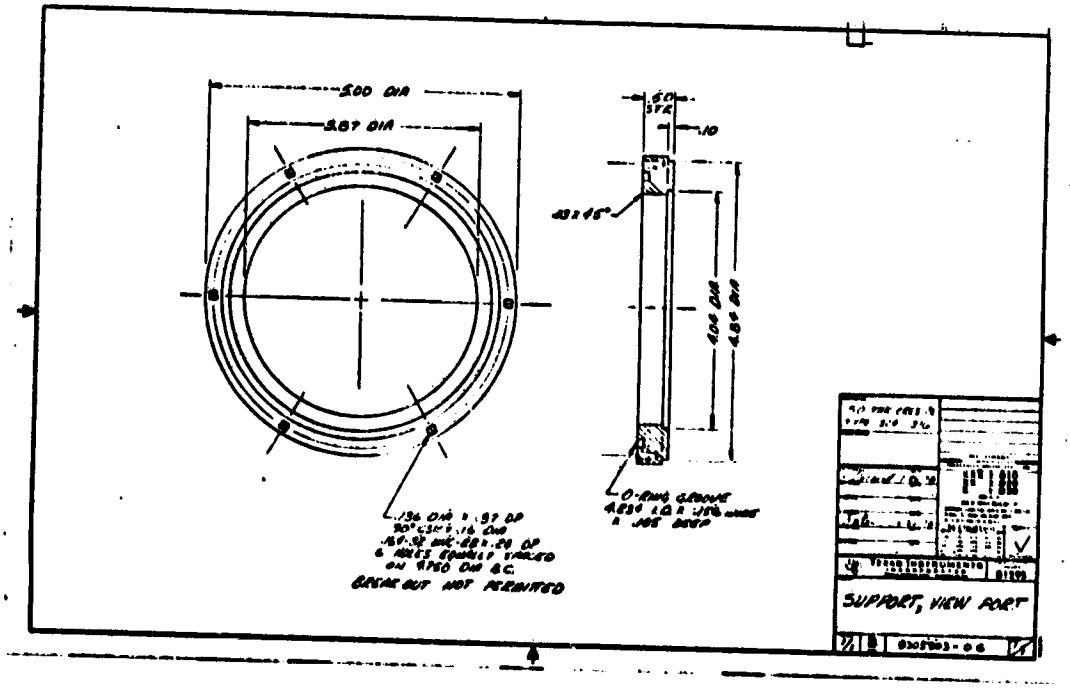
5.00 DIA
3.87 DIA
.10
45°±1°
4.04 DIA
4.09 DIA
.196 DIA x .97 DP
90° CSK x .16 DIA
.257-.27 DIA x .29 DP
6 HOLES EQUALLY SPACED
ON 4.750 DIA B.C.
BREAK OUT NOT PERMITTED
O-RING GROOVE
SUPPORT, VIEW PORT

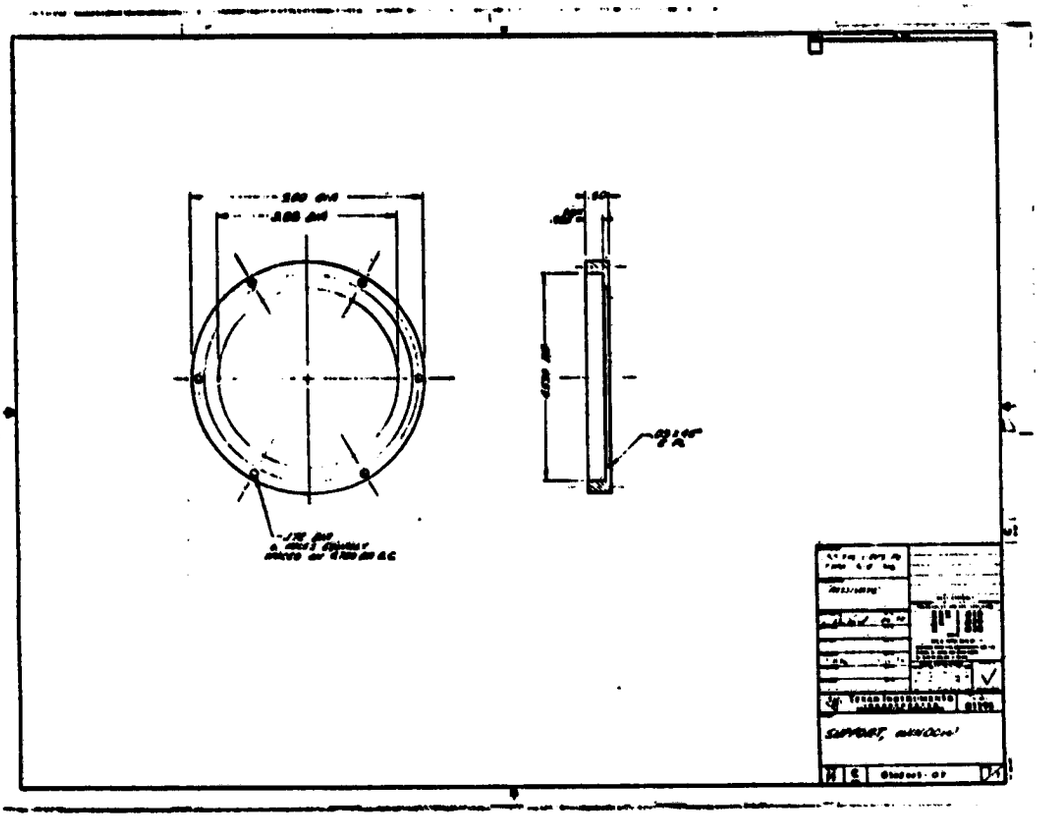

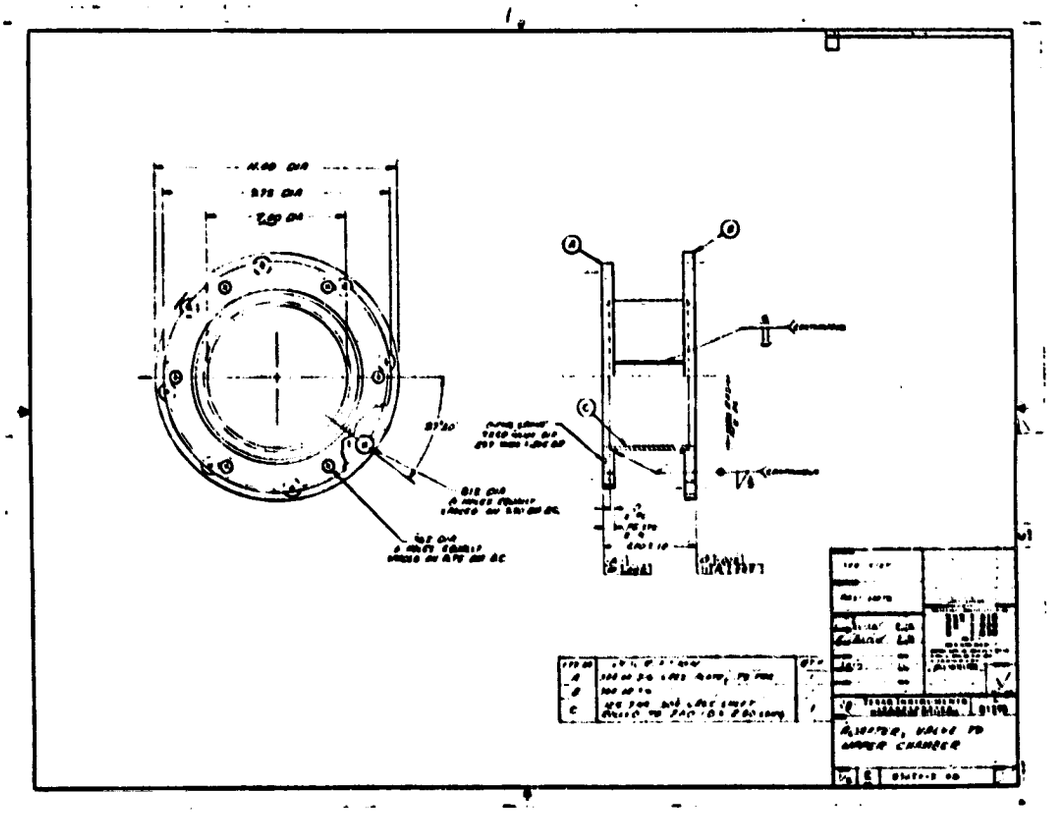

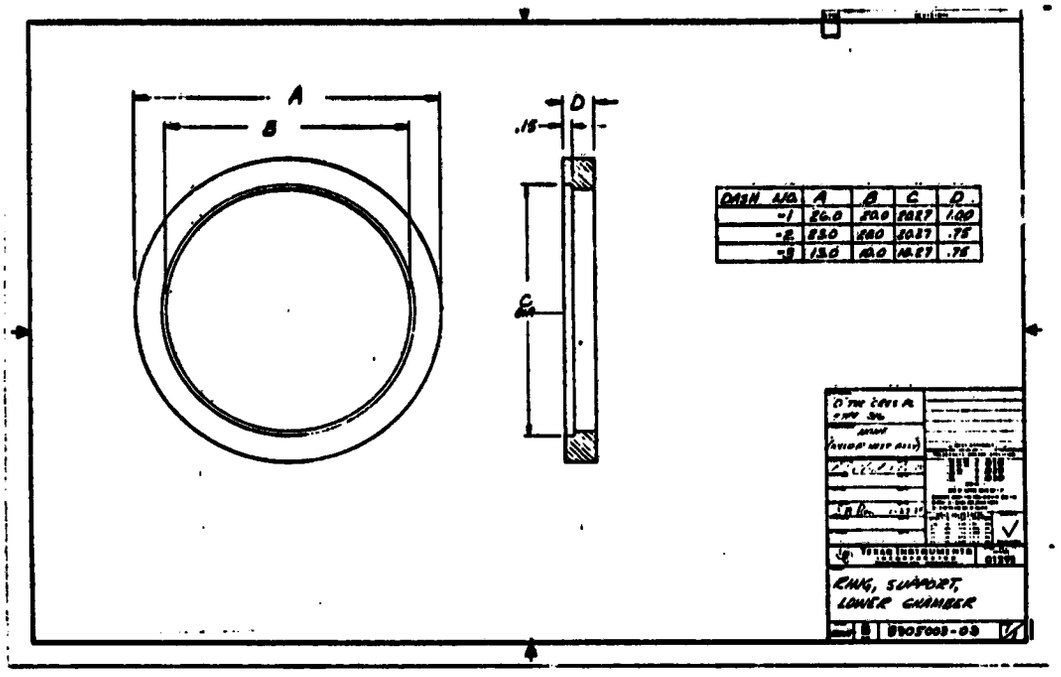
A
B
D
.15
C
DASH NO. | A | B | C | D
-1 | 86.0 | 80.0 | 10.87 | 1.00
-2 | 83.0 | 80.0 | 10.87 | .75
-3 | 13.0 | 10.0 | 10.87 | .75
RING, SUPPORT, LOWER CHAMBER
8905003-03

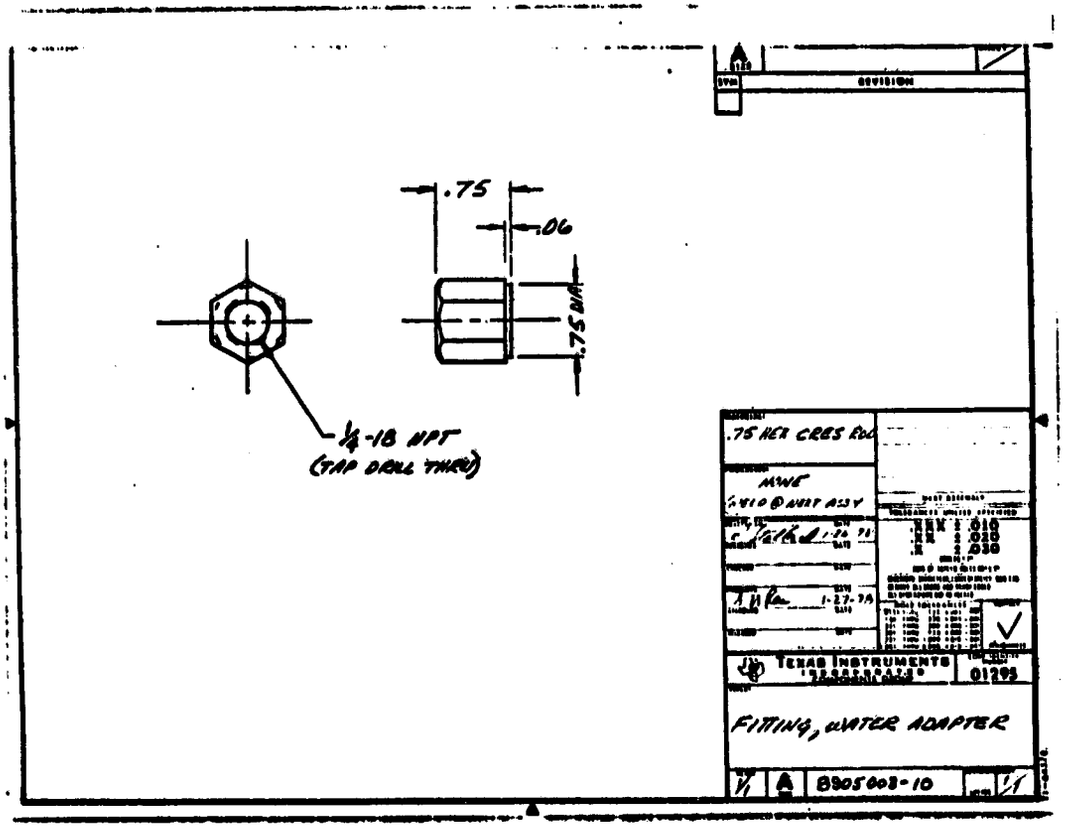
.75
.06
.75 DIA
1/4-18 NPT
(TAP DRILL THRU)
.75 HEX CRES BAR
MWE
1-27-78
TEXAS INSTRUMENTS
01295
FITTING, WATER ADAPTER
A
8905003-10

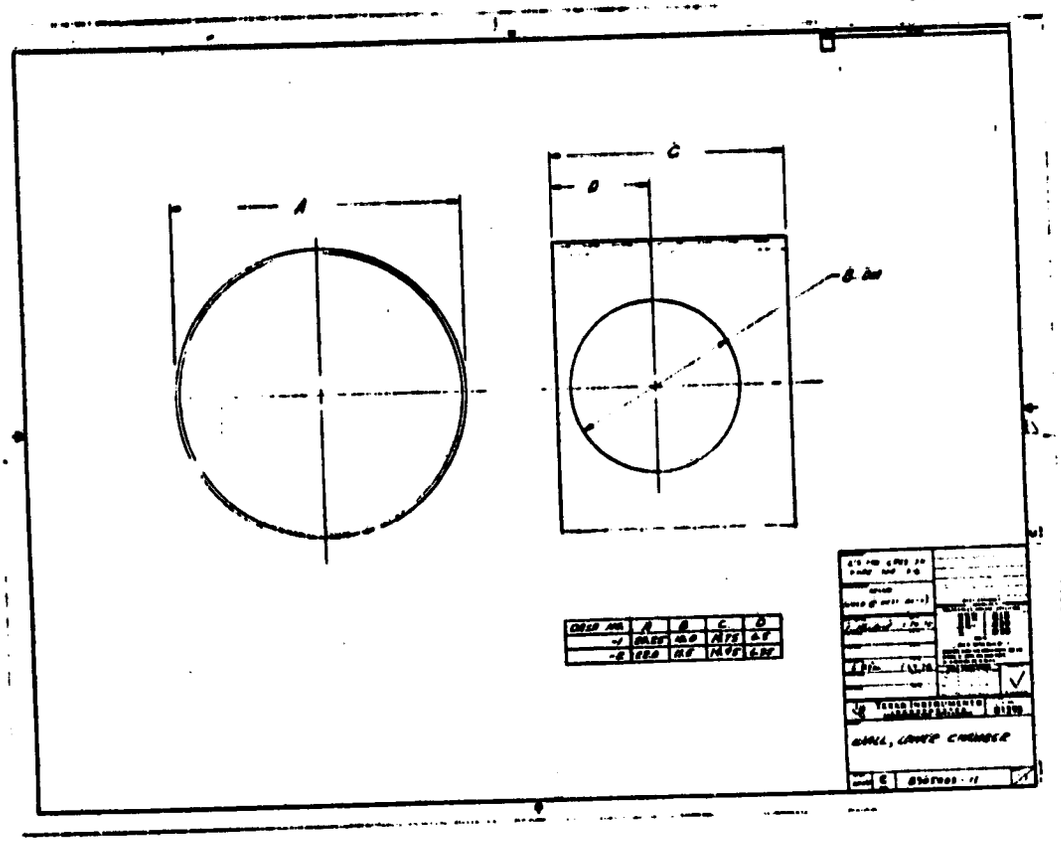
A
C
D
SHELL, LOWER CHAMBER

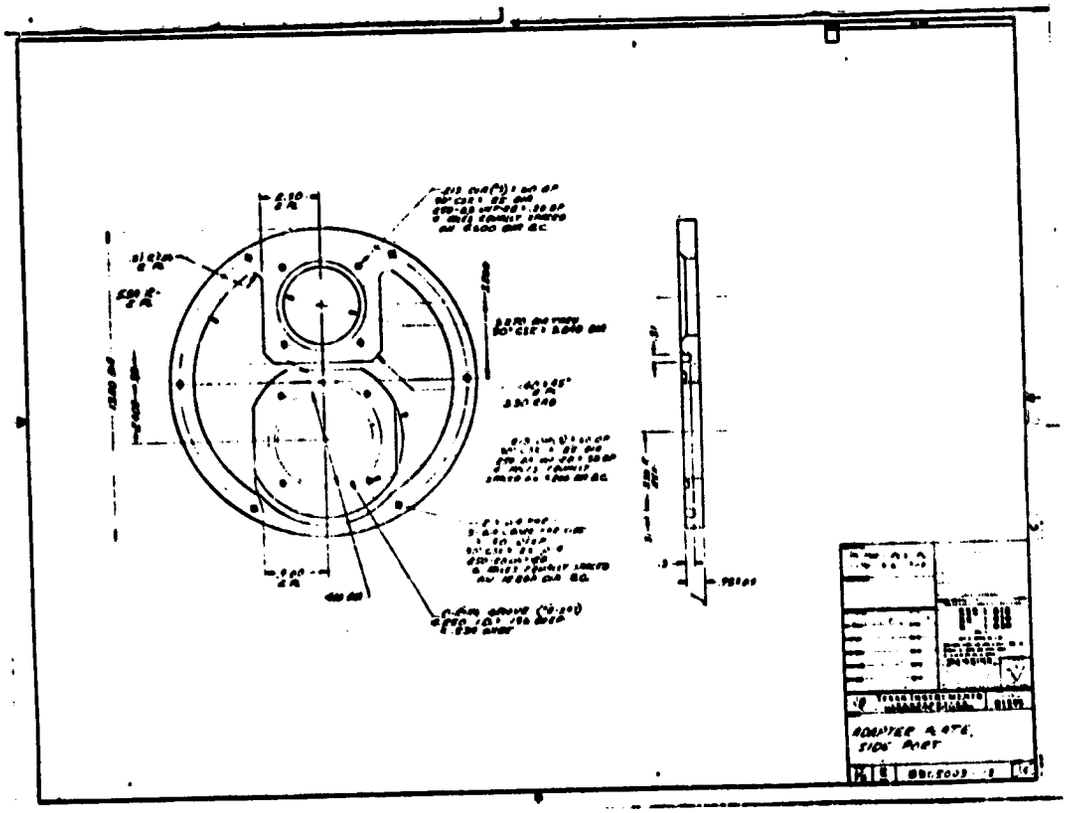
ADAPTER PLATE, SIDE PORT

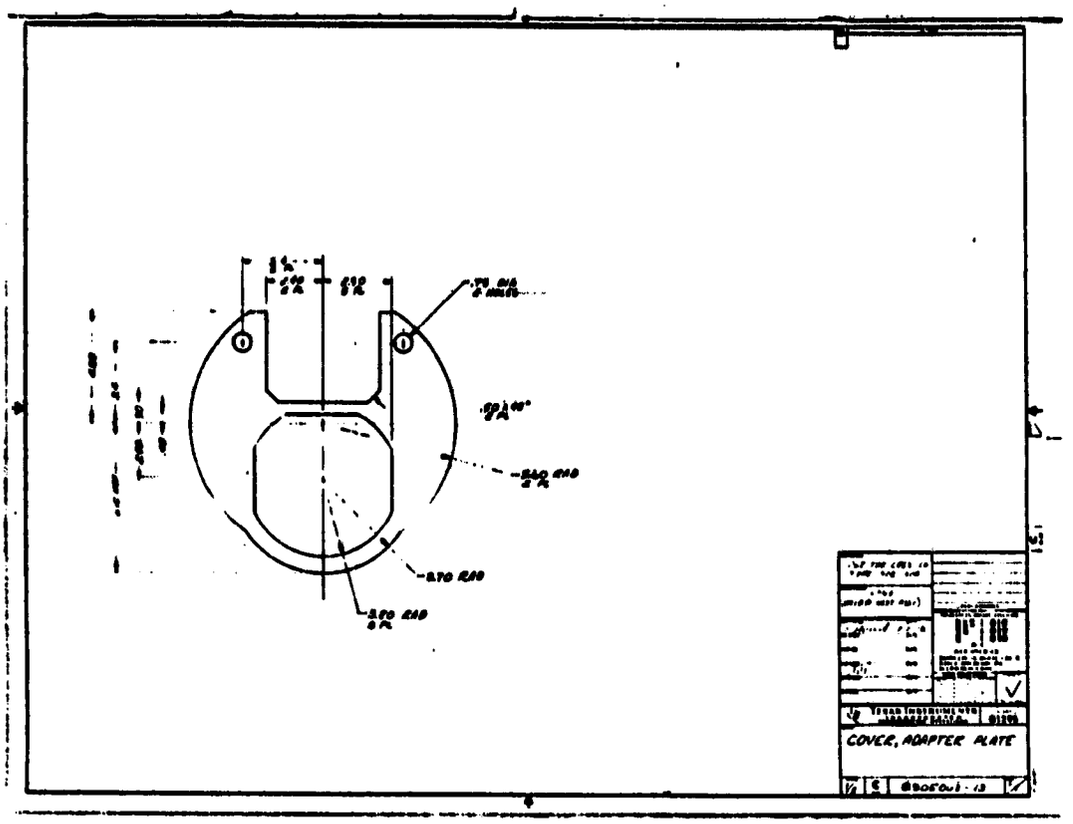
COVER, ADAPTER PLATE

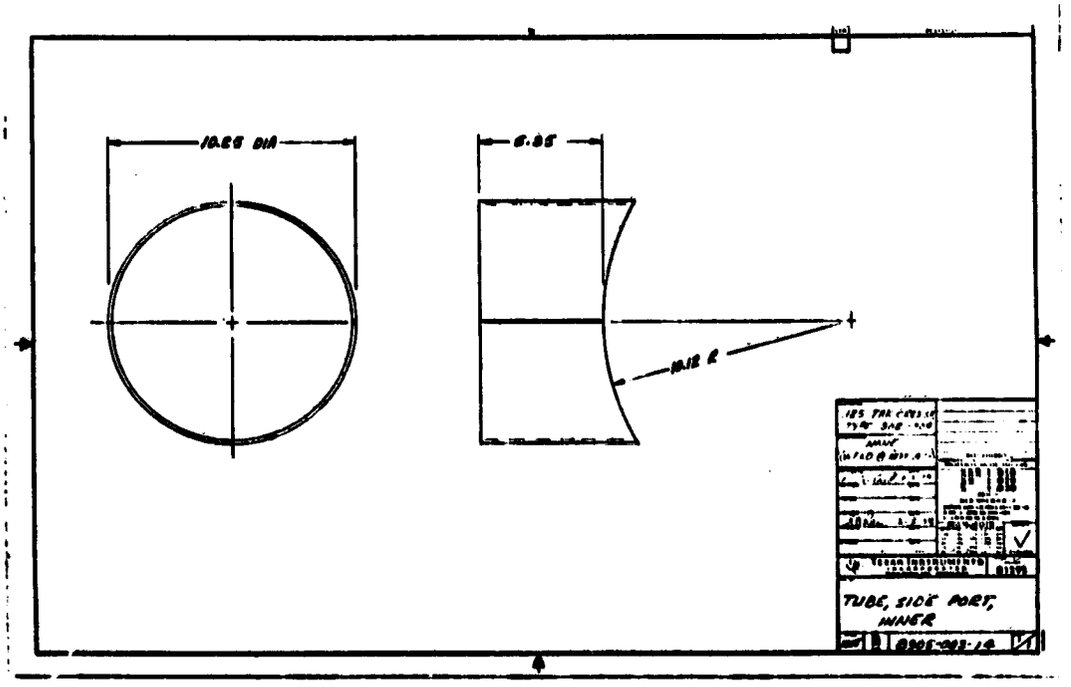
10.65 DIA
6.85
TUBE, SIDE PORT, INNER

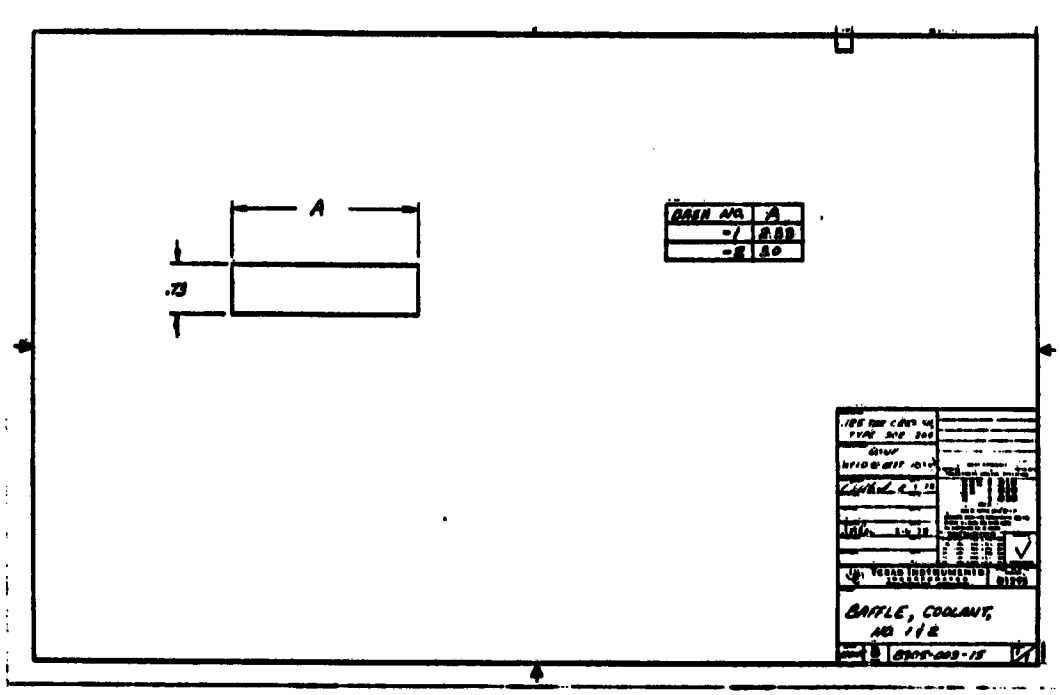
A
.73
BAFFLE, COOLANT, NO 1 & 2
8905-003-15

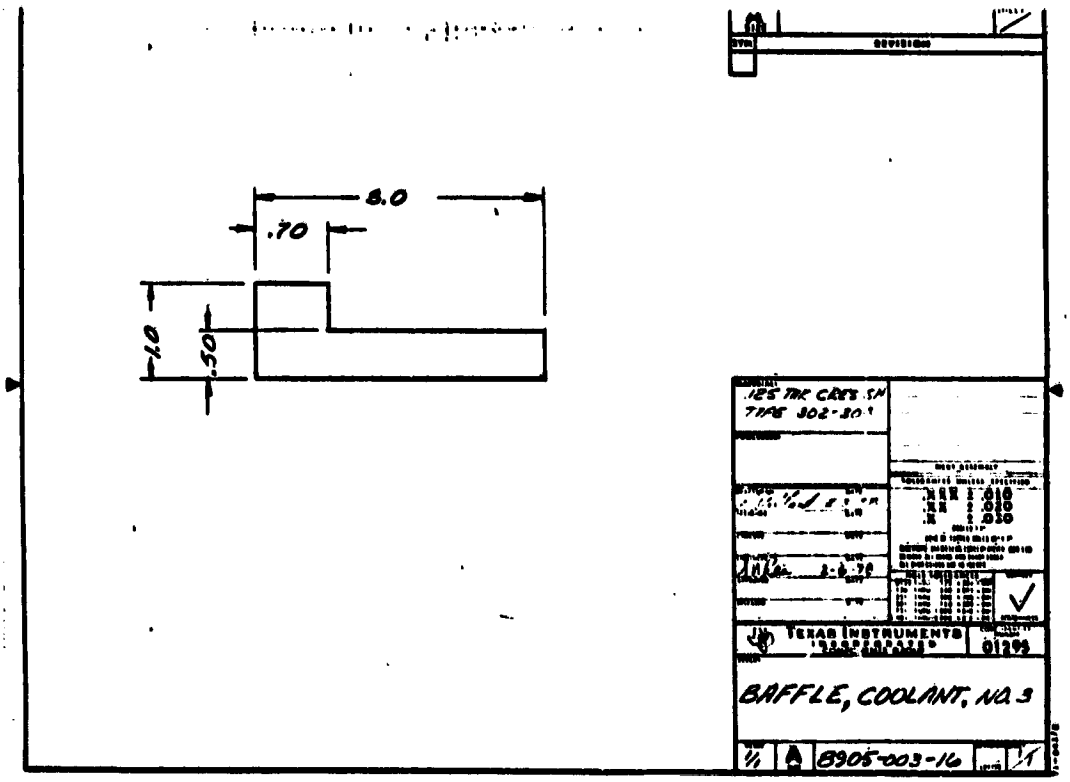
8.0
.70
1.0
.50
.125 THK CRES SH
TYPE 302-304
TEXAS INSTRUMENTS
01295
BAFFLE, COOLANT, NO 3
8905-003-16

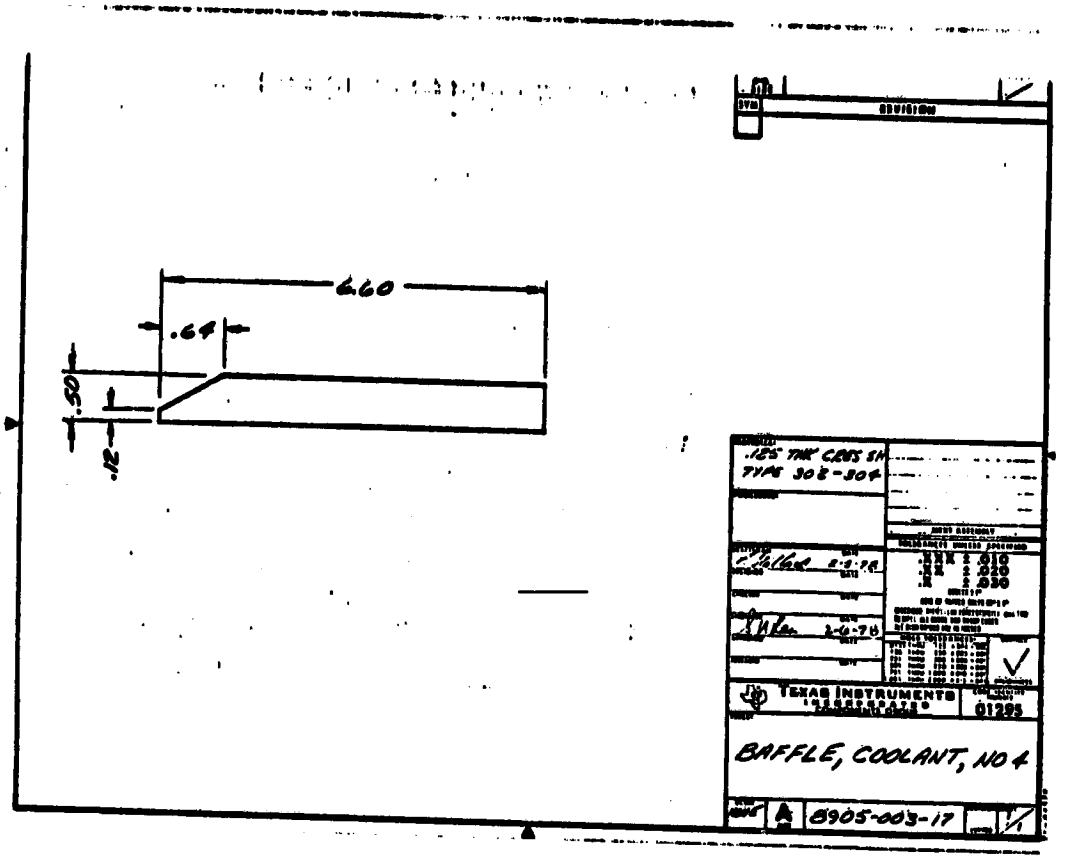
4.60
.64
.50
.12
.125 THK CRES SH
TYPE 302-304
TEXAS INSTRUMENTS
01295
BAFFLE, COOLANT, NO 4
8905-003-17

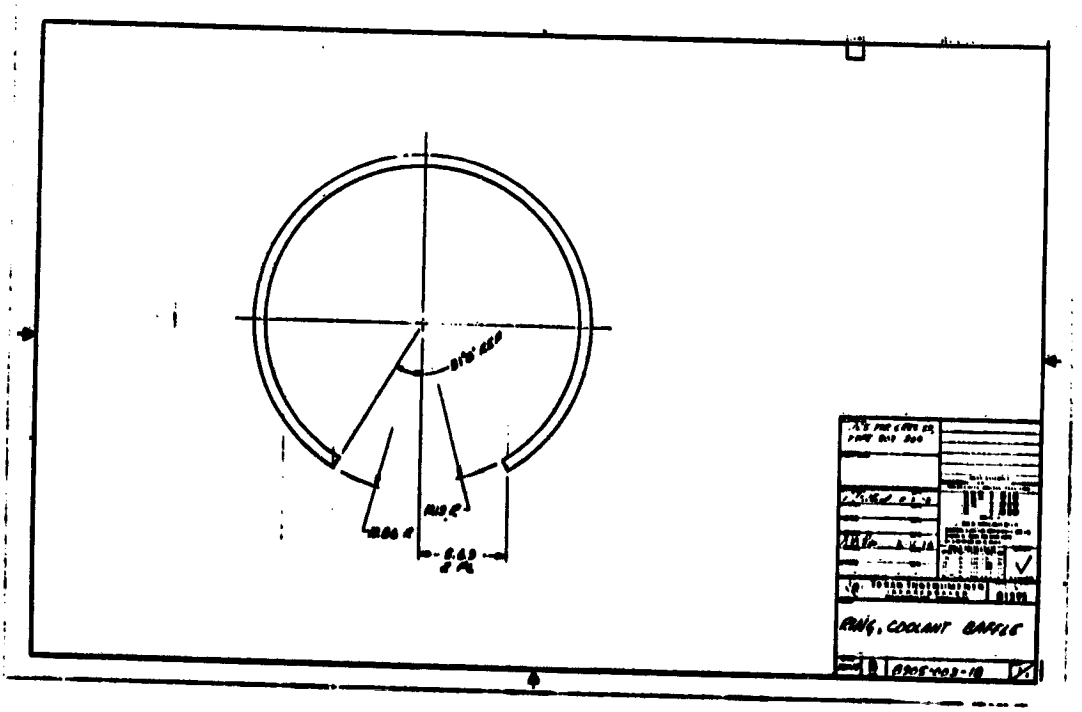
RING, COOLANT BAFFLE

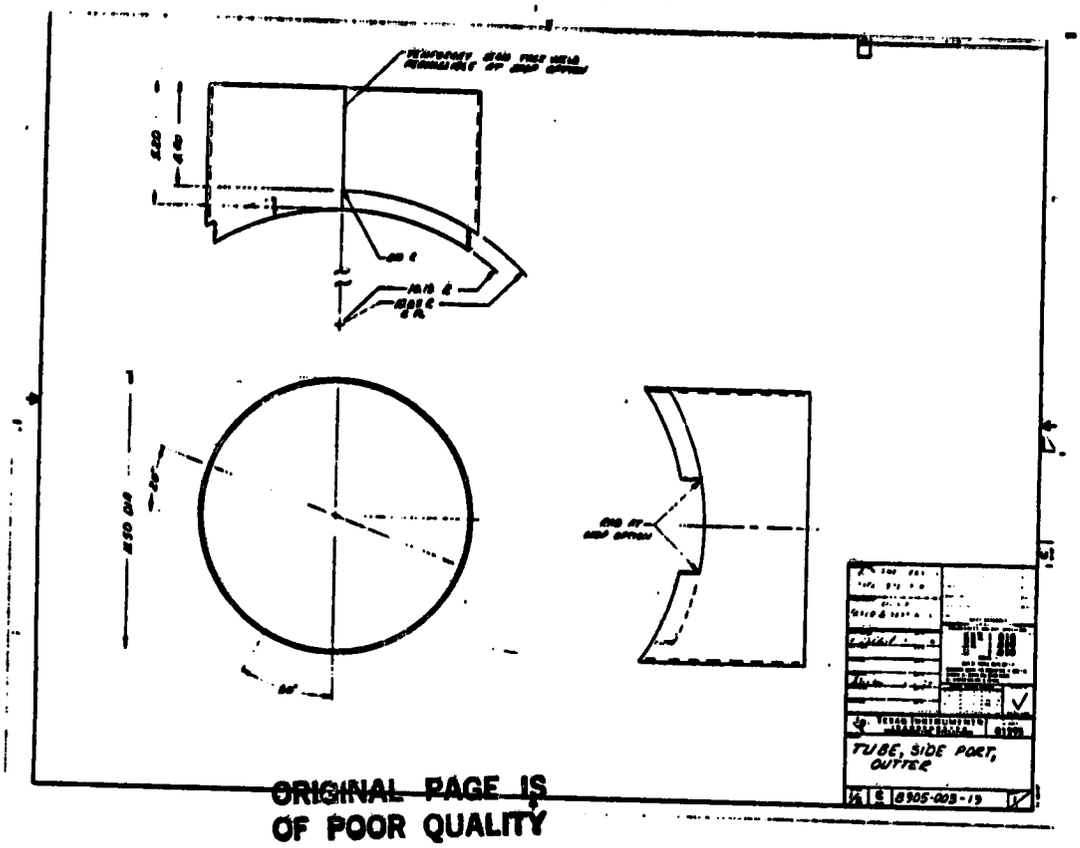

ORIGINAL PAGE IS
OF POOR QUALITY

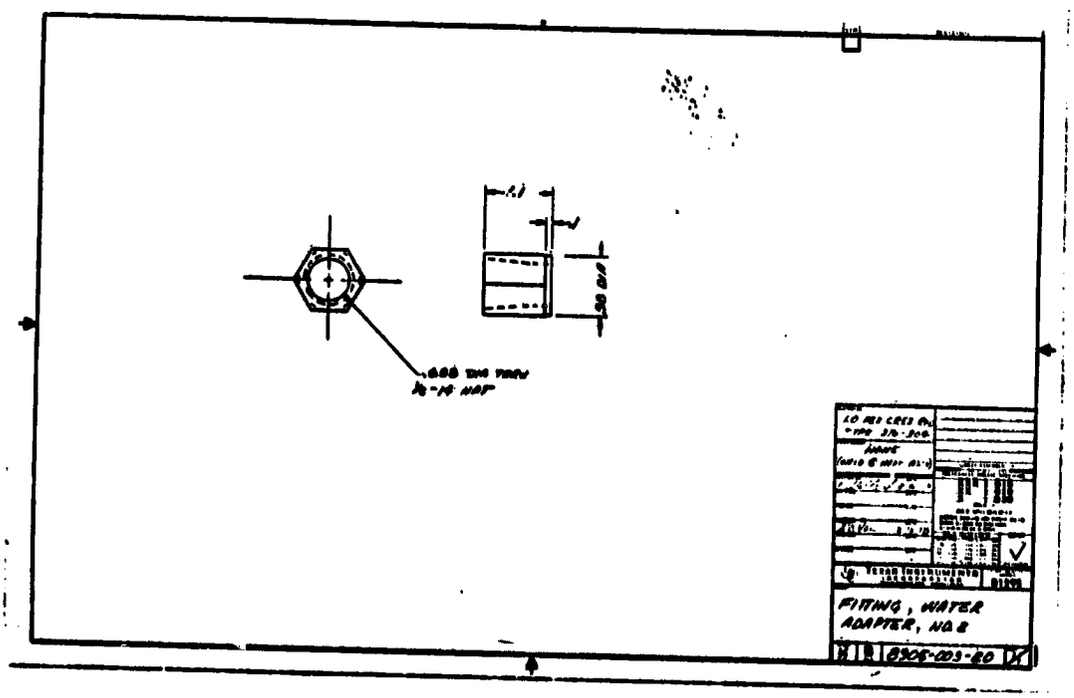

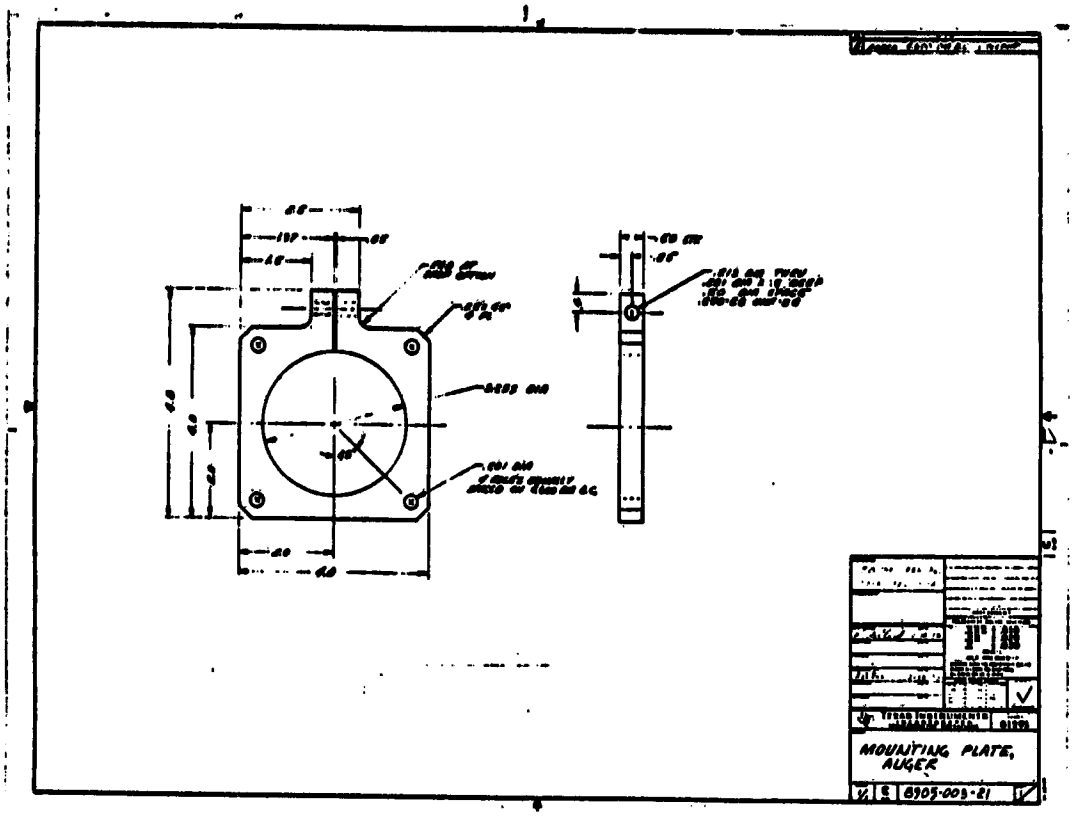
MOUNTING PLATE, AUGER
8905-003-21

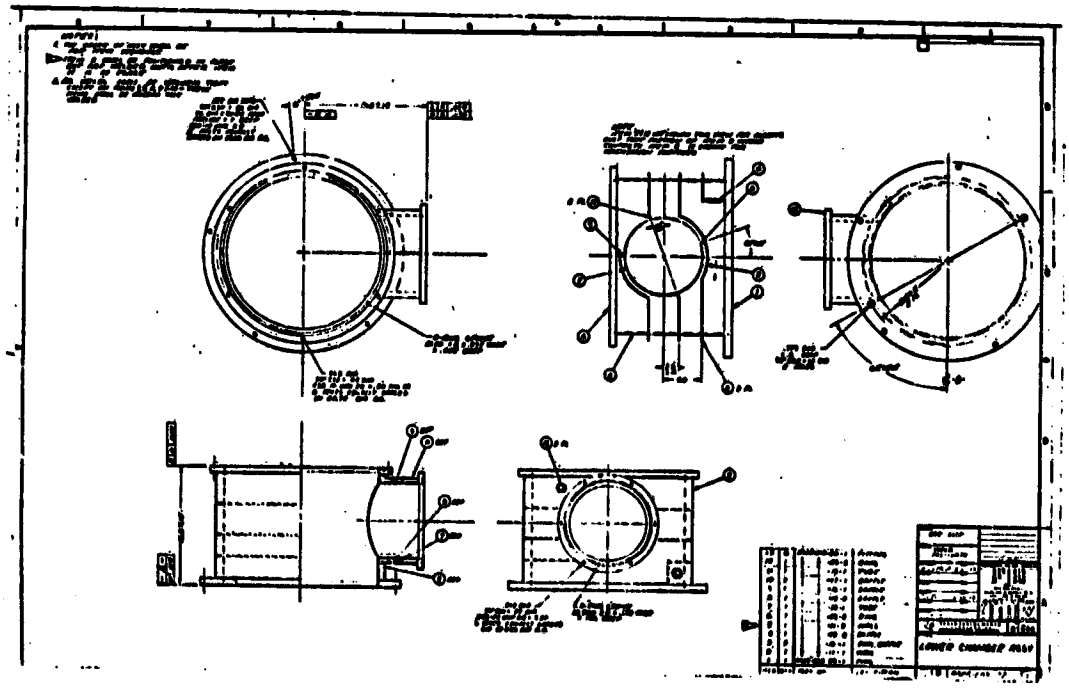

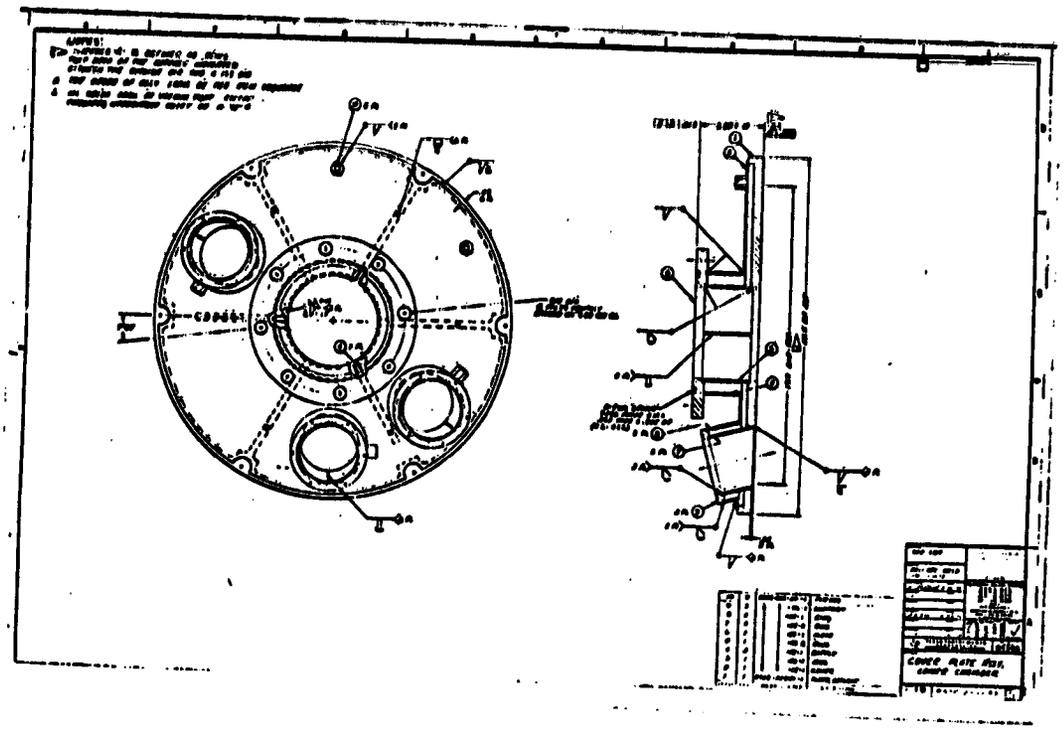

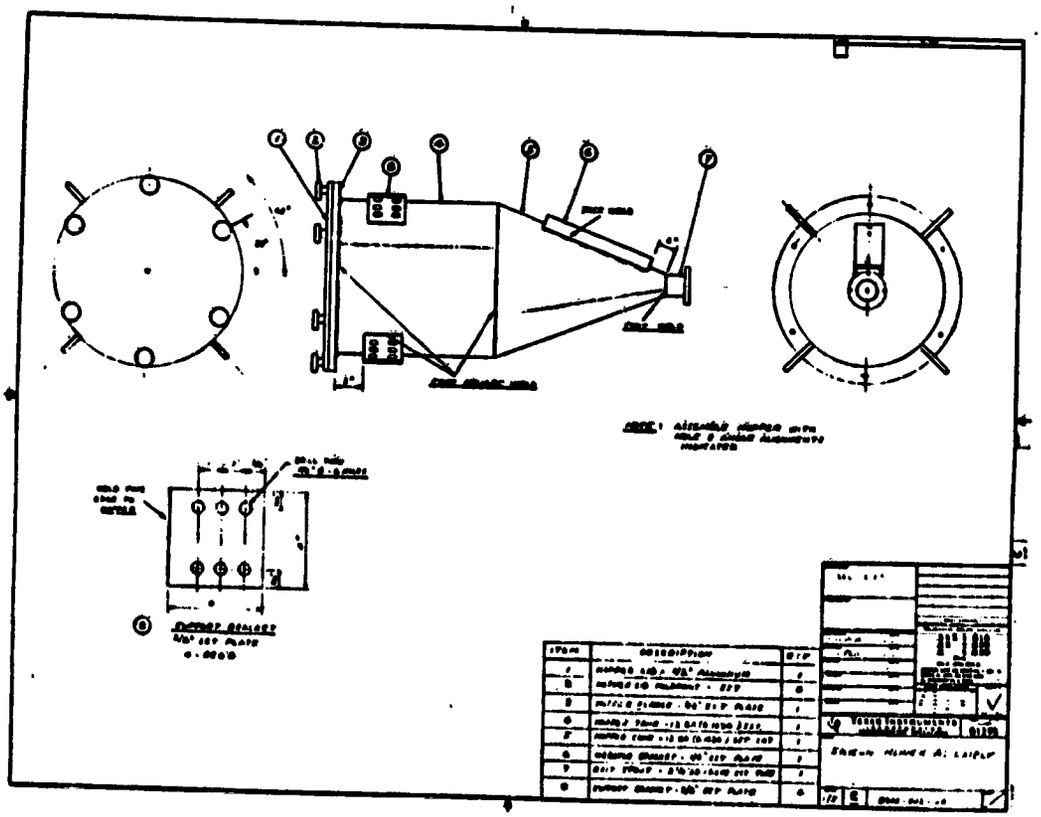

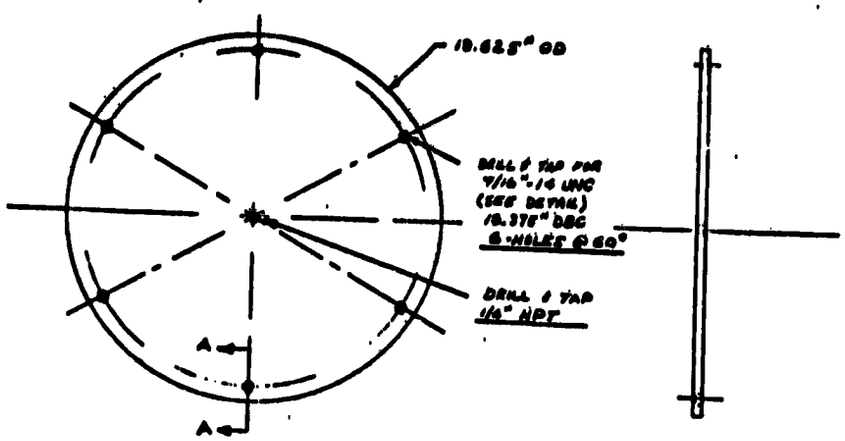

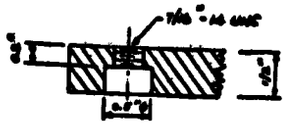

DETAIL A-A

①

1 - REQ'D.
HOPPER LID
MAT'L: 1/2" AL PLATE
8305-002-01
S.N. REA - 4K 2334
12/21/77

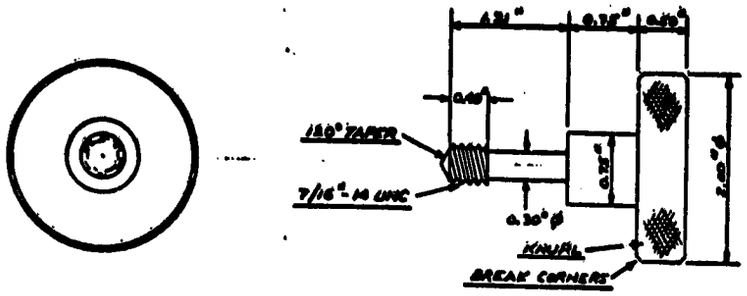

ADVANCED CZ PULLER
HOPPER LID HOLDOWNS
MAT'L: 316 S.S.
NO. REQ'D. 1 6

②

8305-002-02
S.N. REA
11-28-77
4K 2334

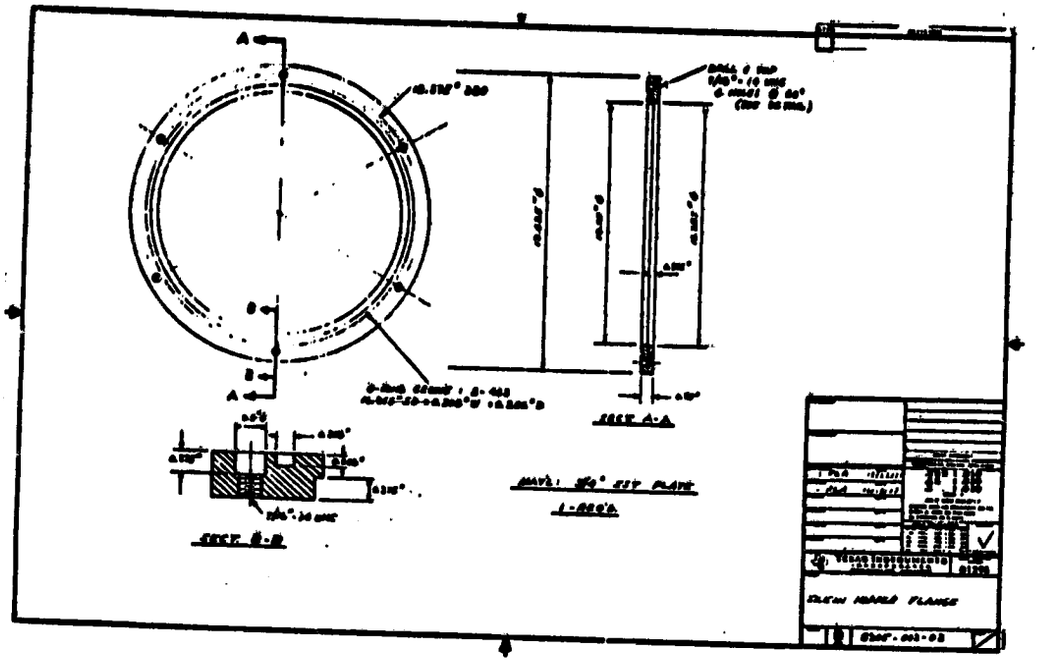

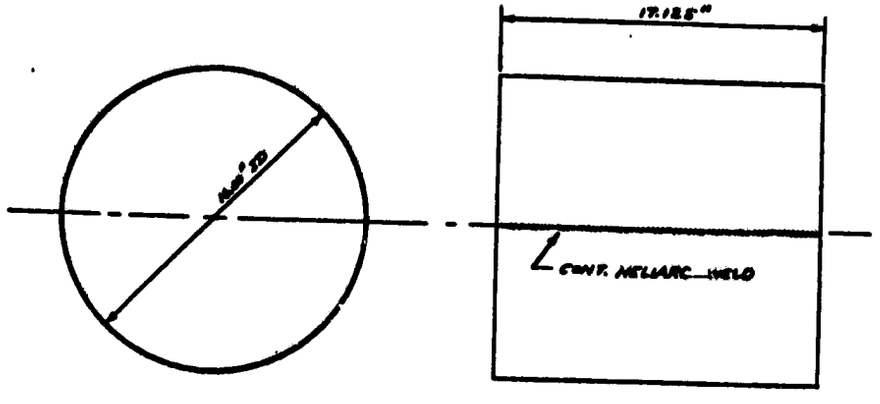

HOPPER TANK
MATL: 12GA SST SHEET
1-REQ'D.
8305-002-04
SN. REA - RT. 3334
12/22/77

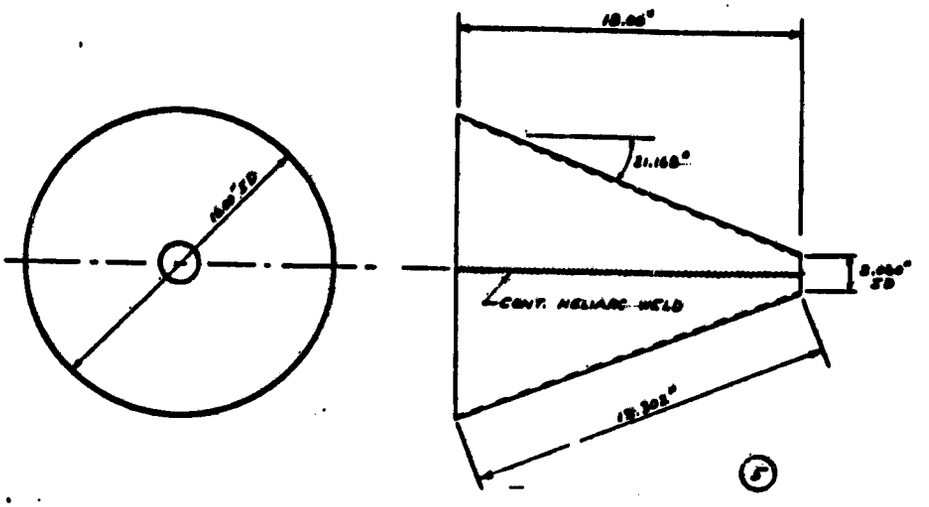

⑤

HOPPER CONE
MAT'L: 12 GA S.S. SHEET
1 - REQ'D.
0302-002-02
S.N. RCA - ST. 3336
12/12/77

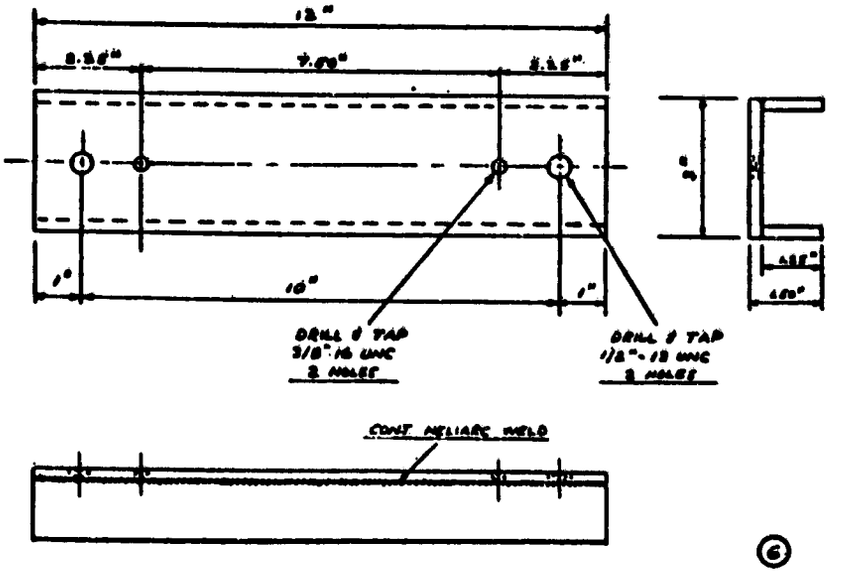

⑥

VIBRATOR BRACKET
MAT'L: 1/4" S.S. PLATE
1 - REQ'D.
0305-002-06
S.N. RCA - ST. 3336
12/12/77

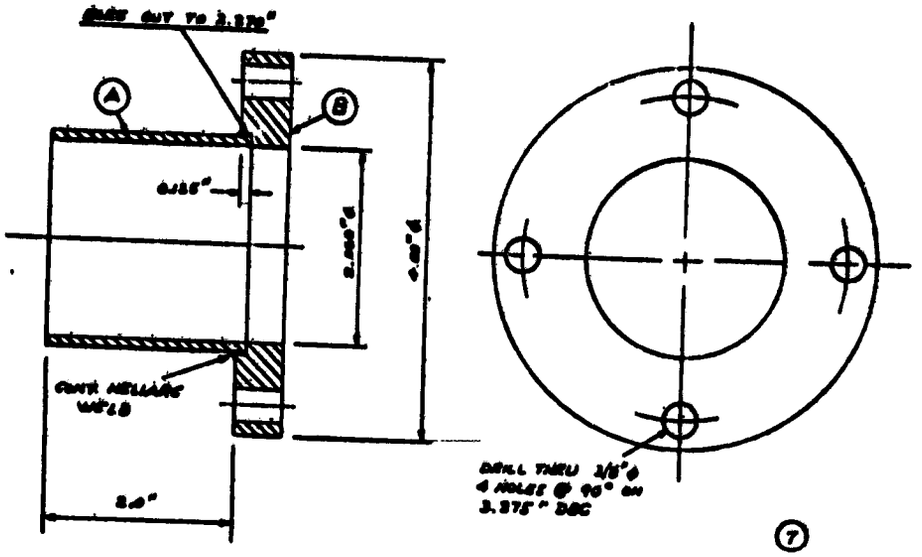

Ⓐ 2 ½"OD × 0.065" WALL SST TUBING
Ⓑ ½" SST PLATE

⑦
HOPPER EXIT SPOUT
1-REQ'D
9905-002-07
S.N. 88A - thru 8334
12/21/77

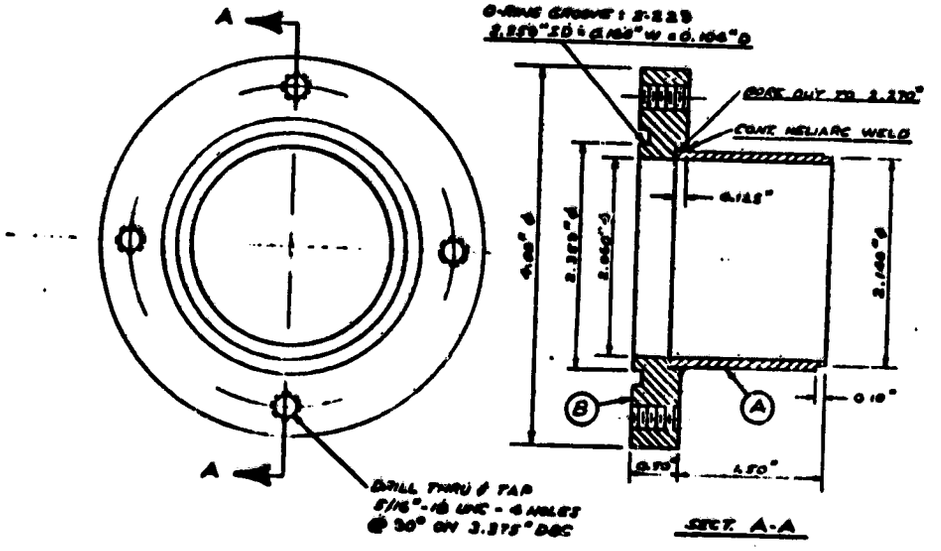

SECT. A-A

Ⓐ 2 ½"OD × 0.065" WALL SST TUBING
Ⓒ NOMINAL 1/2" SST PLATE

ADVANCED EZ FILLER
SI HOPPER TRANSITION
1 REQ'D
S.N. 88A
thru 8334
12-8-77

APPENDIX B

ECONOMIC MODEL BACKUP

CONTINUOUS CZOCHRALSKI ECONOMIC MODEL

CRYSTAL GROWTH EQUIPMENT COST
20-kg Hot Zone

1.	Basic Furnace	$110,000
2.	Auxiliary Melter/Power Supply	3,000
3.	Silicon Hopper/Feed System	4,000
4.	Melt Level Control	5,000
5.	Vacuum Valve	4,000
6.	Contingency	4,000
	Total	**$130,000**

CONTINUOUS CZOCHRALSKI ECONOMIC MODEL
20-kg Crucible, 20-kg Crystals

CYCLE TIME

Event	Time	
1. Cleanup	0.5 h	
2. Load and Melt (10 kg)	2.5	
3. Seed and Top	1.0	
4. Growth (20 kg)	10.9	109 cm
5. Taper (1 kg)	1.0	
6. Unload	0.5	
7. Repeat – 4 Crystals	53.6	436 cm
8. Cool-down	2.0	
TOTALS:	72.0 h	545 cm
Polysilicon Charged:	106 kg	
Power Consumption: (2 h X 80 kW + 67 h X 60 kW)	4180 kW-h	

CONTINUOUS CZOCHRALSKI ECONOMIC MODEL

CRYSTAL GROWTH OPERATING SUPPLIES COSTS
20-kg Hot Zone

	Item	Cost/Run
1.	Crucible Shaft	$ 18
2.	Graphite Crucible	40
3.	Quartz Liner	175
4.	Graphite Shaft Parts	9
5.	Graphite Heater	20
6.	Miscellaneous Graphite Heater Parts	4
7.	Graphite Heat Shield	25
8.	Graphite Felt Insulation	3
9.	Outer Stainless Heat Shield	5
10.	Miscellaneous Heat Shield Parts	6
11.	Shaft Seals	1
12.	Auxiliary Heater	10
13.	Auxiliary Crucible	10
14.	Crystal Seeds	25
15.	Vacuum Pump Filter	9
16.	Vacuum Pump Oil	3
17.	Argon	175
	Total	$538/run